Forest Ecology and Management 504 (2022) 119764

Contents lists available at ScienceDirect

Forest Ecology and Management

journal homepage: www.elsevier.com/locate/foreco

Previous wildfires and management treatments moderate subsequent fire severity

C. Alina Cansler [a,*], Van R. Kane [a], Paul F. Hessburg [a,b], Jonathan T. Kane [a], Sean M. A. Jeronimo [a,c], James A. Lutz [d], Nicholas A. Povak [e], Derek J. Churchill [f], Andrew J. Larson [g]

[a] School of Environmental and Forest Sciences, University of Washington, Box 352100, Seattle, WA 98195-2100, United States
[b] USDA-FS, Pacific Northwest Research Station, 1133 N. Western Avenue, Wenatchee, WA 98801-1229, United States
[c] Resilient Forestry LLC, Seattle, WA, United States
[d] Wildland Resources Department, S.J. & Jessie E. Quinney College of Natural Resources and the Ecology Center, Utah State University, 5230 Old Main Hill, Logan, UT 84322-5230, United States
[e] USDA-Forest Service Pacific Southwest Research Station, 2480 Carson Road, Placerville, CA 95667-5199, United States
[f] Forest Health and Resiliency Division, Washington Department of Natural Resources, MS 47037, Olympia, WA 98504-7037, United States
[g] Department of Forest Management, W.A. Franke College of Forestry and Conservation, University of Montana, 32 Campus Drive, Missoula, Montana 59812, United States

ARTICLE INFO

Keywords:
Burn severity
Mixed-conifer forest
Prescribed fire
Thinning
Reburning

ABSTRACT

We investigated the relative importance of daily fire weather, landscape position, climate, recent forest and fuels management, and fire history to explaining patterns of remotely-sensed burn severity – as measured by the Relativized Burn Ratio – in 150 fires occurring from 2001 to 2019, which burned conifer forests of northeastern Washington State, USA. Daily fire weather, annual precipitation anomalies, and species' fire resistance traits were important predictors of wildfire burn severity. In areas burned within the past two to three decades, prior fire decreased the severity of subsequent burns, particularly for the first 16 postfire years. In areas managed before a wildfire, thinning and prescribed burning treatments lowered burn severity relative to untreated controls. Prescribed burning was the most effective treatment at lowering subsequent burn severity, and prescribed burned areas were usually unburned or burned at low severity in subsequent wildfires. Patches that were harvested and planted <10 years before a wildfire burned with slightly higher severity. In areas managed within 5 years after an initial fire, postfire harvest and planting reduced prevalence of stand-replacing fire in reburns. However, overall, postfire management actions after a first wildfire only weakly influenced the severity of subsequent fires. The importance of fire-fire interactions to moderating burn severity establishes the importance of stabilizing feedbacks in active fire regimes, and our results demonstrate how silvicultural treatments can be combined with prescribed fire and wildfires to maintain resilient landscapes.

1. Introduction

1.1. Background

Fire regimes in many seasonally-dry, temperate forest ecosystems have been altered by past grazing, harvest, and fire suppression (Table 1 of Hagmann et al., 2021 and references therein). This has resulted in a fire deficit in forested landscapes throughout the western US (wUS, Lutz et al., 2009; Haugo et al., 2019; Parks et al., 2015b), relative overabundance of high-severity fire (Haugo et al., 2019; Mallek et al., 2013; Parks and Abatzoglou, 2020), and increasingly large high-severity patches (Cansler and McKenzie, 2014; Stevens et al., 2017). Strong relationships between increased annual drought and increased large fire frequency, greater burned area, and higher fire severity have been documented in temperate forests of western North America (western North America, Holden et al., 2018; Littell et al., 2009; Parisien et al., 2020; Parks and Abatzoglou, 2020; Westerling, 2016). These relationships, along with observed and projected increases in drought and fuel aridity, support the observation that fire regimes in forested ecosystems of western North America are will increase in fire frequency, area burned, and fire severity (Abatzoglou and Williams, 2016; Vose et al., 2018). Hence, the major question for fire researchers and forest

* Corresponding author.
E-mail address: acansler@uw.edu (C.A. Cansler).

https://doi.org/10.1016/j.foreco.2021.119764
Received 27 March 2021; Received in revised form 30 September 2021; Accepted 2 October 2021
Available online 1 November 2021
0378-1127/

managers today is how can they adapt forest landscapes to these rapidly changing fire regimes?

Past management (Agee and Lolley, 2006; Agee and Skinner, 2005; Hessburg et al., 2015; Schwilk et al., 2009) and prior fires (Parks et al., 2015a; Prichard et al., 2017; Stephens et al., 2009; Stevens-Rumann et al., 2016) influence the spread, intensity, and severity of subsequent fires. Silviculture and fire, including both prescribed and wildfire, are thus the main tools that managers can use to restore ecological resilience and resistance, and direct ecosystems toward conditions that will be more resilient under future climates (Hessburg et al., 2021; Millar et al., 2007; Schuurman et al., 2020). In the inland Pacific Northwest the composition, structure, pattern, and functions of low and mid-elevation forests have changed since EuroAmerican colonization (Hessburg et al., 2015, 2005, 2000; Hessburg and Agee, 2003). Throughout this region, the early 21st century correspondingly featured rapidly changing burn conditions. A century of fire exclusion – which continues to be a primary management response – has created a severe fire deficit in historically fire-frequent and moderately fire-frequent forests (Haugo et al., 2019). As a result, many of these forests are overly dense with high fuel loads, making them susceptible to high-severity burns (Hessburg et al., 2005).

Presently, a larger proportion of the frequent-fire, low and mid-elevation elevation pine and mixed-conifer forests burning with higher severity than would be expected under historically active fire regimes (Haugo et al., 2019). Moreover, recent wildfires are creating large high-severity patches in dry and moist mixed-conifer forests (Cansler and McKenzie, 2014) that had low- or mixed-severity (i.e., a mix of low, moderate, and high burn severity burn patches) fire regimes prior to Euro-American colonization (Agee, 1998, 1996). Consequently, broad-scale plans to increase forest resilience and resistance to future wildfires and climatic changes through management (e.g., WADNR, 2020) have been developed. Plans recommend either restoring historical forest structural and species composition patterns, or modifying historical conditions using future climate projections to re-establish resilient forest conditions that match future climates (Churchill et al., 2013; Hessburg et al., 2019, 2021; Prichard et al., 2021). Needed now is specific information about how past management and fire history now influence wildfires under the modern climate (Coen et al., 2018; Haugo et al., 2019; Kane et al., 2019; Mallek et al., 2013). Improved knowledge on the types and influence longevities of effective silvicultural and fire treatments can increase consensus on strategies that can successfully promote resilience and adapt forests to future climates.

We examined determinants of burn severity for fires that burned from 1985 to 2019 in northeastern Washington State, USA. We considered drivers of burn severity and their interactions across a range of management treatments, reburn histories, annual climatic conditions, landscape positions, and forest communities. Our research questions were to identify: 1) co-factors controlling burn severity in untreated long-unburned and reburned areas; and 2) discover the influence of prefire and postfire forest management treatments on burn severity of later wildfires.

2. Methods

2.1. Study area definition

Our study area focused on state, federal and tribally managed lands within the Northern Cascades ecoregion and the Okanogan Highlands ecoregion of Washington State, USA. It included lands managed by the US Forest Service (i.e., Okanogan-Wenatchee NF and the Colville NF), the National Park Service, Confederated Tribes of the Colville Reservation, and the Washington State Departments of Fish and Wildlife (WDFW), and Natural Resources (WA DNR). These ecoregions contain a broad range of biogeoclimatic settings including shrub-steppe, grassland, and sparse woodland communities at lower elevations (approximately 250 m to 1500 m); woodlands and dense pine and mixed-conifer forests at middle elevations (approximately 350 m to 2900 m); and subalpine forests, parklands, and alpine heathlands at the highest elevations (approximately 700 m to 3000 m).

Fires occurred in dry, moist, and cold forest types—as mapped by the Landfire program (Fig. 1)—from the lower to upper montane reaches of the Cascade Range and Kettle River Range, which vary by dominant tree species, historically active fire regimes, precipitation, temperature, climatic water deficit, and evaporative demand placed on tree establishment and growth (Table 1). Elevational gradients in northeastern Washington are steep, and the topography is complexly dissected, especially in the most western parts of our study area (Cansler and McKenzie, 2014), such that the local climate, dominant species, forest structural condition, and fire history can vary over relatively short distances.

Table 1

Summary of potential vegetation groups (PVGs) within the eastern Washington study area, their dominant coniferous species, and 30-yr climate normals. Climate variables are mean annual temperature (MAT; °C), mean annual precipitation (MAP; mm), annual climatic water deficit (DEF; mm), and annual evapotranspiration (AET; mm), for the period 1981–2010. Quantiles are P_{50} [P_{25}, P_{75}]. Table reporduces climatic summaries from Povak et al. (2020a).

PVG	USFS PVT[1]	Fire regime[2]	Dominant species	MAT[3]	MAP3	DEF[3,4]	AET[3,4]
Dry-mixed conifer	Dry Douglas-fir Dry Mixed Conifer Ponderosa pine	Frequent, low-severity surface fire	*Pinus ponderosa* *Pseudotsuga menziesii* *Abies grandis* *Pinus contorta*	6.6 [5.3,7.8]	667 [536,828]	290 [212,337]	255 [235,283]
Moist-mixed conifer	Moist Mixed Conifer Cedar/Hemlock	Mix-severity fire	*Pseudotsuga menziesii* *Pinus ponderosa* *Abies grandis* *Thuja plicata* *Tsuga heterophylla* *Pinus contorta*	6.5 [5.6,7.2]	884 [773,942]	270 [207,301]	258 [237, 285]
Cold-dry conifer	Mtn hemlock-Cold/Dry Subalpine fir-Cold/Dry	Infrequent, high-severity surface and crown fire	*Pinus contorta* *Abies lasiocarpa* *Tsuga mertensiana* *Tsuga heterophylla* *Pseudotsuga menziesii*	3.7 [2.8,4.6]	848 [710,1023]	148 [121,226]	266 [233, 317]

[1] See Table 2.1 in Burcsu et al. (2014) for detailed descriptions of each PVT
[2] Agee (Agee, 1996)
[3] PRISM Climate Group, URL… [4] Appendix A

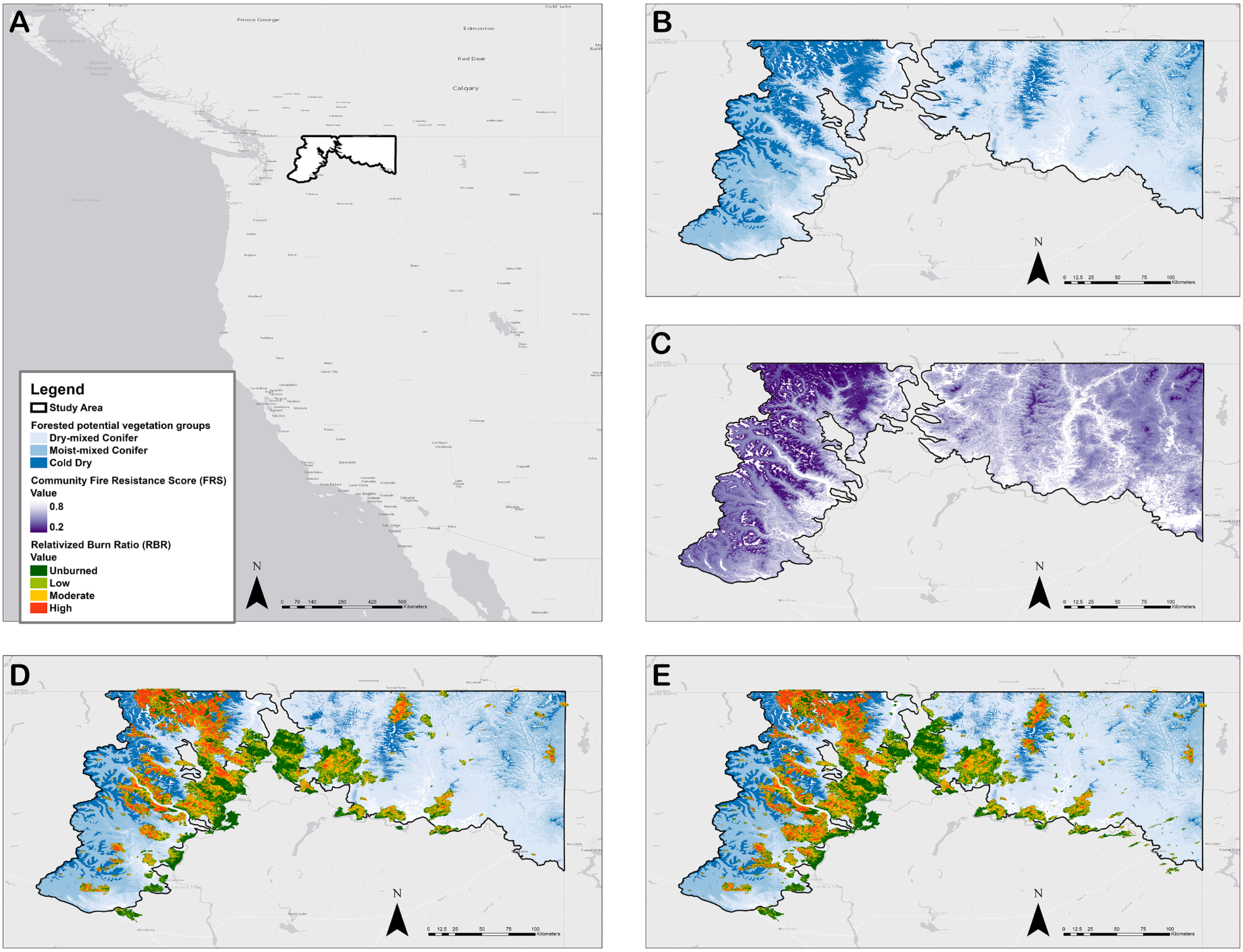

Fig. 1. Maps of study area in northeastern Washington State, USA. (A) The study area was in eastern Washington in North Cascades and Okanogan Highlands ecoregions. (B) We also restricted our analysis forested potential vegetation groups (i.e., dry-mixed conifer, moist-mixed conifer, and cold-dry conifer groups described in Table 1). (C) The community fire resistance score (FRS; Stevens et al. 2020) captures broad-scale gradients in conifer tree species community composition, as reflected in species' fire adapted traits, across the study area. (D) Response data were classified Landsat-based burn severity, as measured by the Relative differenced Burn Severity Ratio (RBR) within fires occurring from 2001 to 2019, with at least 40 ha in conifer forest, and where there were at least 5 MODIS burn detections. (E) Burn severity of fires from 1985 to 2000, and from all fires from 2001 to 2019, including those that were not included as a response, are shown here. These fires were included as predictors in the models predicting the severity of reburns when they predated another fire. Our response data (D) included most, but not all, of the area burned since 1985 (E).

2.2. Response data

2.2.1. Burn severity

We spatially attributed our burn severity response variable for all sampled wildfire burned areas using Landsat derived Relativized Burn Ratio data (RBR; Parks et al., 2014). Fire perimeters from the WA DNR, as corroborated by the US National Monitoring Trends in Burn Severity (MTBS) program (Eidenshink et al., 2007) were used to identify all mapped perimeters for areas that had burned between 1985 and 2019, and burn severity spatial patterns within all fire perimeters were mapped, for a total of 437 fires occurring across 35 years (Fig. 1c). The use of RBR (Parks et al., 2014) provided a relatively accurate measurement of wildfire effects, which in our experience improved spatial accuracy over the commonly-used RdNBR index, especially in the low to moderate range of burn severities (Furniss et al., 2020; Parks et al., 2014). We calculated RBR in Google Earth Engine (GEE) using composites of prefire and postfire images, following the methods of (Parks et al., 2018b) based on the updated GEE script dated July 2021 (Parks, 2021).

Because very low and very high RBR values may be caused by reflectance errors, we removed extreme values below and above the 0.5 and 99.5 percentiles (i.e., <-114 and >605 reflectance values, respectively) of all observed RBR values before analysis. For interpretation and predicting reburn severity, we transformed RBR to three fire response classes; high, low-moderate, and unburned refugia (Table 2). Note that based on how our unburned class is defined, it likely captures ephemeral fire refugia, which only last through a single fire, and persistent fire refugia, which remain unburned or are altered little through multiple fires (Meddens et al., 2018). These classes were calculated based on the average class threshold across fires in the Pacific Northwest and Northern Rocky Mountains, provided in Table 3 of Parks et al. (2014), which were derived from field measurement of burn severity using the Composite Burn Index (Cansler and McKenzie, 2012; Key, 2006). For interpretation, we also provide thresholds for 2% and 98% mortality in Table 1, based on data from Saberi and Harvey (2021), and regression methods in Saberi (2019) and Saberi et al. (2020).

All data used to model burn severity response were from fires that took place between 2001 and 2019, which reflects our improved ability to accurately map fire spread using MODIS satellite data beginning in

Table 2
Fire effects response classes and estimates of percent basal area loss derived from RBR, identified based on Parks et al. (2018b). Two additional thresholds related to tree basal area loss were supplied by Saberi et al. (2020) based on field data from fires in the Pacific Northwest region, USA, and statistical methods (zero and one inflated beta regression) described in Saberi (2019).

Burn severity class	RBR range	Composite Burn Index	Estimated % basal area loss
Burn severity classes modeled with random forest			
Refugia	< 69	0–0.1	< 23 (13–37)
Low-moderate	≥ 69 & < 332	0.1–2.25	≥ 23 (13–37) & < 88 (77–98)
High	≥ 322	>2.25	≥ 88 (77–98)
Additional burn severity thresholds for data interpretation			
All trees survive	< −31		< 2.0 (0.025 – 5.8)
Stand replacing fire	≥ 453		≥ 98 (94–100)

about 2001 (Parks, 2014). We limited response data to forested pixels (i.e., dry-mixed conifer, moist-mixed conifer, and cold-dry conifer potential vegetation groups described in Table 1), with at least 40 ha in forest, and where there were at least 5 MODIS burn detections. We considered a fire to be a "reburn" if any fire burning between 2001 and 2019 fire burned an area previously burned in a fire occurring between 1985 and 2018. Burn severity of fires burning from 2001 to 2019 comprised the response variable dataset for reburns. This resulted in a total response sample from 150 fires, 138 of which had sufficient samples to analyze wildfire effects on long-unburned areas, and 65 of which allowed reburn sampling; 53 fires had separate areas included in both the long-unburned and reburn analysis.

2.3. Predictor data

2.3.1. Temporally varying predictors

Day-of-burning for each sample location (e.g., a 30-m pixel; defined further below in the *Statistical Methods* section) was estimated using MODIS satellite data via the interpolation method of Parks (2014). Any fires with fewer than five MODIS observations (the minimum needed for the Parks (2014) method) were excluded. After estimating the day of burning for each sample in each fire, we acquired daily weather data from gridMET (Abatzoglou, 2013). Daily fire weather variables included spatially interpolated observations based on weather station data (e.g., vapor pressure deficit, wind speed), as well as derived indices related to fire behavior (e.g., energy release component, 1,000-hour fuel moisture) (Table 3). During exploratory analyses, we assessed variables both measured on the day of the burn, and as a five-day average (two days on either side of the estimated burn day), but few differences between approaches were found, and hence we used day-of-burn observations.

Annual climate variables for the period 1981 to 2010 were obtained from the Parameter-elevation Regressions on Independent Slopes Model (PRISM; https://prism.oregonstate.edu/; Daly et al., 2008, 2002, 1994) by averaging monthly data in the year leading up to each fire. Climate variables included precipitation, mean temperature, minimum monthly vapor pressure deficit, and maximum monthly vapor pressure deficit (Table 3). We identified climate anomaly years by differencing yearly summaries from the 30-year climate normals.

2.3.2. Spatially varying predictors

Bioclimatic variables can provide as a proxy for existing vegetation and biomass potential (Table 4). We used actual evapotranspiration (AET) and climatic water deficit (deficit) because they are strongly related to vegetation composition (Stephenson, 1998). We calculated them using the Priestley-Taylor equation (Priestley and Taylor, 1972), following methods of Dobrowski et al. (2013). Along with elevation and latitude, the Priestley-Taylor equation uses albedo, solar radiation, relative humidity, and minimum and maximum temperatures to estimate potential evapotranspiration (PET) for a given day of the year. Precipitation, temperature, and relative humidity data, downscaled to 90 m, were obtained from Climate NA version 6.0 (Wang et al., 2016). Full methods are described in Appendix A.

Three potential vegetation groups (PVGs) were used to classify mixed-conifer forests. The forest types (PWG) were: dry mixed-conifer (DMC), moist mixed-conifer (MMC), and cold-dry forests (CDF; Table 1.), which were reclassified from U.S. Forest Service potential vegetation classifications (Burcsu et al., 2014), following classification scheme in Povak et al. (2020a). Tree species fire resistance traits were captured using the fire resistance score (FRS) of Stevens et al. (2020) (Fig. 1). The FRS was developed by combining relativized tree morphology and litter flammability traits of 29 western North American conifers. Morphological traits included bark thickness, plant height, and capacity for self-pruning; litter flammability traits included flame length, percent consumption, and flame duration under documented burn conditions, with higher scores indicating greater resistance (Stevens et al., 2020). The geospatial map of FRS used in this analysis measure the community-scale FRS. It was calculated based on the relative abundance of each species, based on modeled and mapped basal area of each species (Stevens et al., 2020; Wilson et al., 2013).

Topographic variables were calculated using a 30 m resolution digital elevation model (DEM), created from a 1/3 arc second (approx. 10-m) DEM from the USGS 3DEP program, resampled to 30 m grids to match the resolution of our other data. Variables included a topographical position index (TPI) calculated at 500 m and 2000 m scales, slope, and aspect (Table 4; McGaughey, 2021). We also included topographic variables in initial models that have been shown to be predictors of fire refugia in the neighboring western Cascades as a function of vegetation composition and structure, short-term fuel moisture, and wind exposure (Meigs et al., 2020).

We used imputed 30-m rasters of forest structure variables (Table 4) from the Landscape Ecology, Modeling, Mapping and Analysis program (https://lemma.forestry.oregonstate.edu; LEMMA) to approximate basal area, canopy cover, quadratic mean diameter of trees, and a diameter diversity index for the year 2000, the start of our study period. These forest structure variables were interpolated across the landscape based on field-sampled regional inventory plots and the canonical relationships between the plot data and several wall-to-wall Landsat imagery datasets, using the gradient nearest neighbor (GNN) imputation procedure described in Ohmann and Gregory (2002).

2.3.3. Reburns: Fire history and severity predictor data

All fires in the burn severity atlas (1985 – 2019) were used to establish fire history for the period (Fig. 1e; Table 4). For all burn severity response data where a previous fire had burned since 1985, we calculated time since the last fire, maximum previous severity (maximum RBR), and the number of previous fires. Areas that had burned two or three times between 1985 and the most recent fire (e.g., twice and thrice reburned) were excluded from the analysis due to low sample sizes.

2.3.4. Management history

Areas where silvicultural or fuel management treatments had occurred from 1991 to 2017 were identified using the U.S. Forest Service-Forest Activity Tracking System (FACTS) database (https://data.fs.usda.gov/geodata/edw/datasets.php). We first condensed FACTS database treatments into four broad categories: prescribed fire, mechanical thinning, planting, and timber harvest. In locations where more than one of the four treatment categories occurred, we considered the combined treatments as separate categories (e.g., we also assessed "thinning and harvest", "harvest and planting", "prescribed fire and harvest", and "prescribed fire, harvest, and planting"). Prefire planting primarily occurred within two non-adjacent timeframes, so we divided the prefire planting into "old" (≥20 years before the fire) and "recent" (≤10 years before fire) categories. There were limited observations of

Table 3
Spatially-varying predictor variables used in final Random Forest machine leaning models to predict burn severity. Methods for calculating AET and CWD normals are described in Appendix A.

Variable	Expected relationship with fire severity	Modeling steps used	Units or range	Description and methods	Grain (m)	Citation
Bioclimatic setting						
Actual evapotranspiration climate normals (AET)	Increase	Removed during variable reduction	mm	Actual evapotranspiration is related to the amount of photosynthesis that can actually occur, given water imputes and soil conditions. Calculated following methods described in Appendix A. Variable represent the 30-year mean actual evapotranspiration.	90	Appendix A
Climatic water deficit normals (deficit)	Decrease	Removed due to multicollinearity	mm	Climatic water deficit represents the amount of evaporative demand that cannot be met because soil water has been depleted during the summer dry period. Calculated following methods described in Appendix A. Variable represent the 30-year mean 30-year mean climatic water deficit	90	Appendix A
Community fire resistance score (FRS)	Increase	Final model	continuous numeric	A single fire resistance score for all mature trees at a location, calculated used community-weighted averaging of species' traits to estimate the fire resistance scores of different forest communities, using interpolated species distribution and relative abundance data.	30	Stevens et al. (2020)
Potential vegetation group (PVT)	Lowest in DMC, highest in CDF.	Removed due to multicollinearity	Dry mixed conifer (DMC), moist mixed conifer (MMC), cold-dry forests (CDF)	Potential vegetation groups: Dry mixed conifer (DMC), moist mixed conifer (MMC), cold-dry forests (CDF). These represent climax vegetation types reflecting common species assemblages, site productivity, and disturbance regimes, which could have many different successional states and forest development structures in them.	30	Burcsu et al. (2014)
Topography						
Topographical position index, at 500 m scale (TPI 500)	Highest at large values, which represent local ridgetops that would be more exposed to the wind.	Removed due to multicollinearity	Continuous numeric index	Smaller, negative values represent valley bottoms and depressions, and larger positive values represent ridgetops and hilltops. Calculated using the terrain() function in R's raster package based on a 30 m resolution ground model	30	Hijmans and van Etten (2012)
Topographical position index, at 2000 m scale (TPI 2000)	Highest at middle values, which represent mid-slope positions of large landscape features.	Final model	Continuous numeric index	Smaller, negative values represent valley bottoms and depressions, and larger positive values represent ridgetops and hilltops. Calculated using the terrain() function in R's raster package based on a 30 m resolution ground model	30	Hijmans and van Etten (2012)
Local slope	Increases	Removed due to multicollinearity	radians	Calculated using the terrain() function in R's raster package.	30	Hijmans and van Etten (2012)
Local aspect	Increases	Removed during variable reduction	Cosine transformed radians	Cosine transformed radians. −1 = South, 1 = North, and values near 0 are East and West. Calculated using the terrain function in R's raster package based on the USGS 3DEP ground model resampled to a 30 m resolution to aid processing time	30	Hijmans and van Etten (2012)
Catchment slope	Increases	Final model	radians	Mean slope of the catchment area. Calculate in R's RSAGA package	30	Brenning and Bangs (2016)
Catchment area	Decreases	Removed due to multicollinearity	square meters	Hydrological catchment extent. Calculate in R's RSAGA package.	30	Brenning and Bangs (2016)
Catchment flow path	Decreases	Removed during variable reduction	meters	Length of hydrologic flow path (m). Calculate in R's RSAGA package	30	Brenning and Bangs (2016)
Relative position	Increases	Removed during variable reduction	numeric (0-10)	Relative topographic position (0–10); lower to higher elevation within 500 m radius; captures the landscape position of a given site. Calculate in R's RSAGA package	30	Brenning and Bangs (2016)
Forest structure						
Basal area	Increase	Final model	m^2/ha	Interpolated basal area of live trees >=2.5 cm dbh in the year 2000	25	Ohmann, and Gregory (2002)
Canopy cover	Increase	Removed due to multicollinearity	percent	Interpolated canopy cover of all live trees in the year 2000	25	Ohmann, and Gregory (2002)
Quadratic mean diameter	Increase		cm		25	

(continued on next page)

Table 3 (*continued*)

Variable	Expected relationship with fire severity	Modeling steps used	Units or range	Description and methods	Grain (m)	Citation
		Removed during variable reduction		Interpolated quadratic mean diameter of all dominant and codominant trees in the year 2000		Ohmann, and Gregory (2002)
Diameter diversity index	Decrease	Removed during variable reduction	numeric continuous	Interpolated diameter diversity index in the year 2000. DDI is a measure of the structural diversity of a forest stand, based on tree densities in different DBH classes.	25	Ohmann, and Gregory (2002)

Table 4
Temporally-varying predictor variables used in final Random Forest machine leaning models to predict burn severity. Methods for calculating AET and CWD normals are described in Appendix A.

Variable	Expected relationship with fire severity	Modeling steps used	Units or range	Description and methods	Grain (m)	Citation
Annual antecedent weather anomalies						
Annual precipitation anomaly	Decrease	Removed during variable reduction	mm	The sum of annual precipitation for the 12 months proceeding the July of the fire, minus 1981–2020 normals	4000	Daly et al. (2002) ; http://prism.oregonstate.edu, created 4 Feb 2004.
Annual monthly temperature anomaly	Increase	Final model	C	The average monthly temperature for the 12 months proceeding the July of the fire, minus 1981–2020 normals	4000	Daly et al. (2002) ; http://prism.oregonstate.edu, created 4 Feb 2004.
Annual mean monthly minimum vapor pressure deficit anomaly	Increase	Final model	mm	The average monthly minimum vapor pressure deficit for the 12 months proceeding the July of the fire, minus 1981–2020 normals	4000	Daly et al. (2002) ; http://prism.oregonstate.edu, created 4 Feb 2004.
Annual mean monthly maximum vapor pressure deficit anomaly	Increase	Removed during variable reduction	mm	The average monthly maximum vapor pressure deficit for the 12 months proceeding the July of the fire, minus 1981–2020 normals	4000	Daly et al. (2002) ; http://prism.oregonstate.edu, created 4 Feb 2004.
Daily fire weather						
Burning Index	Increase	Removed during variable reduction	continuous numeric index	The burning index is derived from the spread component (SC), a relative index of rate of fire spread, and the energy release component (ERC), a relative index of the amount of heat released per unit area in the flaming zone of an initiating fire. The BI is expressed as a numeric value related to potential flame length in feet multiplied by 10..	4000	Abatzoglou (2013); also see: https://www.fs.fed.us/rm/pubs_int/int_gtr169.pdf
Energy Release Component	Increase	Removed due to multicollinearity	continuous numeric index	Modeled mean daily energy release component. A relative index of the amount of heat released per unit area in the flaming zone of an initiating fire. with larger values representing greater potential heat release	4000	Abatzoglou (2013); also see: https://www.fs.fed.us/rm/pubs_int/int_gtr169.pdf
Wind Speed	Increase		m/s	Modeled mean daily windspeed	4000	Abatzoglou (2013)
Mean vapor pressure deficit	Increase	Removed due to multicollinearity	mm	Modeled mean daily mass of water vapor per volume of moist air relative to the maximum humidity the air could hold at the same temperature	4000	Abatzoglou (2013)
100-hour dead fuel moisture	Increase	Removed due to multicollinearity	percent	Modeled daily fuel moisture for dead woody surface fuels 2.54–7.62 cm in diameter. 1,000-hour timelag fuel moisture is a good indicator of the severity of a medium term (4- to 6-month) drought event	4000	Abatzoglou (2013); also see: https://www.fs.fed.us/rm/pubs_int/int_gtr169.pdf
1000-hour dead fuel moisture	Increase	Final model	percent	Modeled daily fuel moisture for dead woody surface fuels 7.62–20.32 cm in diameter. 1,000-hour timelag fuel moisture is a good indicator of the severity of a medium term (4- to 6-month) drought event	4000	Abatzoglou (2013); also see: https://www.fs.fed.us/rm/pubs_int/int_gtr169.pdf
Minimum relative humidity	Decrease	Removed due to multicollinearity	percent	Modeled lowest daily mass of water vapor per volume of moist air relative to the maximum humidity the air could hold at the same temperature	4000	Abatzoglou (2013)
Maximum relative humidity	Decrease	Removed during variable reduction	percent	Modeled highest daily mass of water vapor per volume of moist air relative to the maximum humidity the air could hold at the same temperature	4000	Abatzoglou (2013)

planting from 10 to 20 years before fire, so we excluded that time frame from the analysis. We assessed fires occurring from 2001 to 2018, with the start year matching the availability of MODIS fire spread and daily fire weather data, which we used for pairing controls (see below), and 1 year after the latest available FACTS data record at the time of analysis.

We analyzed combinations of treatments and fires occurring in three combinations, with the response variable always being the RBR burn severity of the most recent fire. We identified areas where: (1) treatments occurred before a fire (hereafter, *treatment-fire*, nine types), and (2) treatments occurred before two successive fires (hereafter, *treatment-fire-fire*, two types), and (3) areas where treatment occurred after a first fire (hereafter, *fire-treatment-fire*; three types) but before a reburn (Table 6). *Fire-treatment-fires* were limited to treatments that took place $\leq$ 5 years of the first fire, because we were specifically interested in treatments implemented in response to the fire. Treatment types that did not include at least 550, 30-m pixels (~50 ha) were excluded from analysis. Some prescribed fires were also present in our burn severity atlas. For this analysis, if a prescribed fire occurred before a wildfire, that area analyzed as a *treatment-fire*.

2.3.5. Spatial autocorrelation

We represented spatial autocorrelation using principal coordinates of neighbor matrices analysis (PCNM) (Borcard and Legendre, 2002; Dray et al., 2006). The PCNM procedure uses principal coordinates analysis on a matrix of points within a predefined distance, resulting in eigenvectors that maximize Moran's index of autocorrelation. Low-order vectors represent larger-scale spatial autocorrelation, and high-order vectors represent local-scale spatial autocorrelation (Borcard and Legendre, 2002). We followed methods of Povak et al. (2020b) for application of the PCNM method to predictive modeling of burn severity with random forests (described in the next section). We used truncated distance matrices with a threshold distance of 10,000-m to calculate lower-ordered (1–10) PCNM vectors and included the first six vectors as predictors (Table 5). We refer readers to Povak et al. (2020b), and the associated online supplementary information for a full discussion of how inclusion of PCNM eigenvector decreases spatial autocorrelation of model residuals and explains how they are used as predictors. PCNM eigenvectors were calculated in R using the *vegan* (Oksanen et al., 2019) and *RSpectra* packages (Qiu Y, 2018).

2.4. Statistical methods

2.4.1. Identifying co-factors controlling burn severity in untreated long-unburned areas and reburns

Because burn severity is controlled by a number of drivers that can have non-linear, contingent relationships (Dillon et al., 2020; Kane et al., 2015a, 2015b; Meigs et al., 2020; Povak et al., 2020b), we use random forest (RF) modeling (Breiman, 2001) to predict RBR. For this analysis, we resampled the 30-m scale RBR and associated predictor data with a 270 m grid, and then randomly sampled 20,000 of these 270-m grid cells for modeling. Most of the predictor data is captured at finer native scales (25, 30, or 90-m scale), with the exception of the annual climate and fire weather data, which have a 4-km native resolution. We used this 270 m resampling approach to decrease the influence of fine-scale spatial autocorrelation in our models, and because analyzing every 30-m burn severity pixel was computationally intractable. We chose the 270-m grid size based on explicit testing of a range of sampling scales and recommendations by Povak et al. (2020b), and our observation that a 270-m grid cell adequately samples the unburned class, while decreasing prevalence of fine-scale spatial autocorrelation.

We modeled burn severity in long-unburned areas separately from reburns. Areas that burned where silvicultural and mechanical fuel treatments had occurred were excluded from this analysis and are addressed below in a separate analysis. Each model predicted occurrence of three burn severity classes: refugia, low-moderate severity, and high-severity (Table 2).

We determined predictor variable inclusion in the RF models through a multi-step process, with the goal of identifying a parsimonious variable set that allowed direct comparison of predictors between long-unburned and reburn models. We began by assessing multi-collinearity among predictors prior to variable reduction using Spearman's rank correlations ($r < |0.7|$). Among correlated variables, those with the strongest correlation with continuous values of RBR were retained. Next, we developed an RF model with the reduced set of predictors and a 10-fold cross-validation procedure to identify the best *meta*-parameters and assess model stability and robustness to prediction. In machine learning, *meta*-parameters or hyper-parameters are configurations that are external to the model, but are used to estimate model parameters (Boehmke and Greenwell, 2019), and in RF models these include the number of decision trees in the forest, and the criteria used to split each node. We conducted separate cross-validations for differing burning periods and fires to prevent model overfitting to large fire-spread days and allow for model transferability to other events.

Third, using the identified meta-parameters, we reduced variables in the RF models using backwards stepwise reduction, until we found the minimum model that maintained at least 95% of the cross-validated accuracy of the full model. Based on the variable reduction results for the two models (long-unburned areas and reburns), we selected a final set of predictors, which include the set of predictors for each model, without any highly correlated variables, and at least one variable in each

Table 5
Fire history and spatial autocorrelation predictor variables used in final Random Forest machine leaning models to predict burn severity. Methods for calculating AET and CWD normals are described in Appendix A.

Variable	Expected relationship with fire severity	Modeling steps used	Units or range	Description and methods	Grain (m)	Citation
Fire history						
Time since last fire	Increase	Final model	years	Based on the fire ignition year of the fire	30	Based on data from fire perimeters geospatial layers from the US national Monitoring Trends in Burn Severity (MTBS) program (Eidenshink et al., 2007), WA DNR, and United States Forest Service (USFS)
Previous RBR	Decrease	Final model	numeric index (see Table 2)	Relativized Burn Ratio or previous fire; calculate for all mapped fires since 1985	30	Parks et al. (2018b, 2014)
Spatial autocorrelation						
Principal coordinates of neighbor matrices (PCNM 1–6)	No expectation	Final model (PCNM 1–3); Removed during variable reduction (PCNM 4–6)	numeric continuous	Low-order PCNM vectors represent broad-scale SA, while higher-order vectors represent more fine-scaled SA	30	Borcard and Legendre (2002)

Table 6
Treatment in mixed-conifer forest in Northeastern Washington state that occurred before wildfire. Wildfires and reburns occurred from 2001 to 2019, and treatments took place from 1982 to 2017. In reburns, previous fires occurred from 1985 to 2018.

Treatment	Total area (ha) in class [1]	Total samples (n) [2]	Control samples within environmental range of treated cases (n)	Sub-sample analyzed (n) [3]	Unique fires + burn periods in treated subsample	Unique fires + burn periods in control subsample
Untreated areas						
Untreated wildfires (control)	505,510	69,343	NA	19,254	1,385	NA
Untreated reburns (control)	51,919	7,122	NA	6,313	421	NA
Treatment-fire						
Thinning	427	4,742	11,316	4,742	58	501
Thinning + harvest	429	4,772	9,015	4,772	58	494
Harvest [2]	8,908	98,982	17,505	5,835	942	275
Harvest + planting [2]	2,958	32,864	16,826	5,608	177	623
Planting (old; ≥20 years before fire)	291	3,235	8,521	3,235	61	507
Planting (recent; ≤10 years before fire) [2]	449	4,992	10,193	4,992	26	608
Prescribed fire [2]	2,130	23,670	17,551	5,850	100	511
Prescribed fire + harvest	819	9,101	11,307	9,101	101	720
Prescribed fire + harvest + planting	137	1,524	1,375	1,375	8	128
Treatment-fire-fire						
Harvest + planting	122	1,351	2,290	1,351	29	220
Planting	319	3,544	3,943	3,544	40	285
Fire-treatment-fire						
Harvest	62	690	1,881	690	15	116
Harvest + planting	327	3,632	3,010	3,010	43	318
Planting	1,230	13,664	4,007	4,007	59	306

[1] For untreated areas, the area in the table represents the total burned area represented by the sample, not the area of samples.
[2] Untreated areas were sampled on a 270 m grid, which was then randomly down sampled to 20,000 points. Extreme RBR values above and below the 0.5 and 99.5 percentiles were also trimmed from all datasets.. Treated areas were sample on a 30 m grid, matching the resolution of the RBR data.
[3] To create subsamples either the cases or controls were subsample, based on the best matched environmental variables. For Harvest, Harvest and Planting, Plantings (recent), and Prescribed fire computational limitations required us to subsample both groups before creating matched controls and cases. We subsampled the cases to the listed subsample size, and subsampled the controls to 3 times that amount, then drew environmental matched samples from that subsample.

variable category (Table 3). Fire history variables were not included in models of long-unburned areas. Using this final set of variables, we ran two separate models for both the long-unburned and reburns models: (1) a final cross-validation, with the best *meta*-parameters to determine final cross-validated accuracy and a kappa statistic, and (2) a final model without cross-validation, in which we increased the number of RF trees from 1000 to 5000. Using the latter, we identified final out-of-bag (OOB) error and calculated class probabilities and variable importance.

All analyses were conducted in R version 3.6.3 (2020–02-29, R Core Team, 2020) using the *ranger* package version 0.12.1 (Wright and Ziegler, 2015), and the *caret* package, version 6.0–86 (Kuhn, 2008) for cross-validation and *meta*-parameter tuning, and the *tidyverse* package for data manipulation and visualizations (Wickham et al., 2019). For all RF model runs, we set the sample fraction to take equal samples from each of the predicted burn severity classes within each bootstrap to create balanced random forest modeling conditions (Chen et al., 2004), with the sample fraction of the largest class set to a maximum of 68% of the total sample. For model interpretation, we created one- and two-variable partial dependence plots to assess the correspondence between variables and burn severity, using the *pdp* package in R, version 0.7.0 (Greenwell, 2017). Two-variable whisker plots allowed us to look for interactions and nonlinearities between predictors.

We used class probability predictions for each observation to calculate accuracy statistics for binary classes: refugia vs. non-refugia, low- and moderate-severity vs. other severities, and high- vs. other burn severities. This allowed us to compare model accuracy and direction of errors for fire effects classes for different management priorities. We calculated model accuracy using the area under the receiver operator characteristic curve (AUC, Bradley, 1997), and the confidence interval around the AUC. The AUC provides an average estimate of the discriminatory ability of any model to predict the probability of being in one of two classes, with AUC values ≥ 0.5 indicating better discrimination than by random chance selection (Hosmer et al., 2000). The higher the AUC, the stronger is model discrimination between two classes. We also calculated model sensitivity in several ways. We estimated model sensitivity to identifying:

1) true positives, where (*truepositives*Ã·(*truepositives* +*falsenegatives*)); e.g., for high severity, the proportion of high severity observations correctly predicted),
2) true negatives, where (*truenegatives*Ã·(*truenegatives* +*falsepositives*)); e.g., for high severity, the proportion of unburned or low-moderate severity observations correctly predicted),
3) model positive predictive value (*truepositives*Ã·(*truepositives* + *falsepositives*));; e.g., for high severity, the proportion of predicted high severity that is actually high severity),
4) model negative predictive value (*truenegatives*Ã·(*truenegatives* + *falsenegatives*)); for high severity, the proportion of predicted "not high severity" severity that is actually not high severity), and
5) model overall accuracy (total correct as a proportion of total observations).

We used the package *pROC* version 1.17.0.1 in R (Robin et al., 2011) to calculate accuracy statistics with the 10,000 bootstrap samples used to calculate AUC confidence intervals.

2.4.2. Establishing the influence of prefire and postfire forest treatments on the burn severity of later wildfires

Management treatments (both prefire and postfire) occurred on 3.6% of the total area burned in the study area landscape, across an area burned by 44 unique fires in the interval between 2001 and 2019.

Treatment-fire samples occurred on 3.1% of the once-burned landscape, and *fire-treatment-fire* samples made up 3.0% of the reburned area. Treatments also took place in differing forest types, where treatments that included prescribed fire were primarily conducted in dry frequent-fire forests, and FRS generally exceeded 5.0 (Figure B.4, B.5, and B.6). Because of their small areas, and relatively small sample size (Table 6), we did not include them in the landscape scale modeling. In treated areas, a census of the 30-m pixels (0.09 ha) in all treated areas was compiled. Controls—untreated wildfires and untreated reburns—were drawn from the same dataset as used in the RF modeling above, sampled on a 270-m grid. To assess the impacts of treatments on burn severity, we tested for differences between treated and untreated controls, after subsampling treatment and controls to match bioclimatic setting and fire weather for each treatment type.

To match the distributions of the controls to each treatment type we removed the control observations within fires that were outside the range of the treatment values of FRS, 1,000-hr fuel moisture on the day of burning and mean annual temperate anomalies in the year proceeding the fire. For post-fire pre-reburn treatments, we also matched previous burn severity and time between fires. Next, we used the matchControls function from the *e1071* package, version 1.7–6 in R (Meyer et al., 2020) to subsample the control sample to the treatment sample, using pairwise dissimilarities to match as closely as possible the FRS and 1,000-hr fuel moisture for prefire treatment. For postfire pre-reburn treatments we also matched previous burn severity, and time between fires. Sample sizes varied by treatment types, and for treatments with very large samples (e.g., > 9,000 pixels) we took a random sample of the available data (Table 6), to allow for the "matchControls" to run. For *fire-treatment-fire* samples, where there were more treatment points than control points, we subsampled treatments to match the available controls. We tested for statistical differences between control and treatment distributions using a niche overlap index to quantify the degree of distribution overlap, and two-sided Kolmogorov–Smirnov tests (K–S) (Conover and Iman, 1981; Marsaglia et al., 2003) to test for significant differences. We plotted subsampled treatment and control RBR distributions to visualized differences.

3. Results

3.1. Co-factors controlling burn severity in untreated long-unburned and reburn areas

The final model predicting three classes of burn severity in long-unburned areas had an out-of-bag (OOB) error rate of 0.305 (Table 7). The model performed best at predicting the high severity (AUC = 0.846), and worst at predicting low-moderate severity (AUC = 0.702) outcomes. The final model predicting burn severity in reburns performed better than the model for long-unburned areas, with an OOB error rate of 0.355 (Table 8). The same patterns of higher prediction accuracy for high severity and unburned areas were found within reburns.

The most important predictions in our RF models were related to large-scale gradients across the study area (Fig. 2). Variables measuring the spatial autocorrelation of the burn severity data were strong predictors in both models. Specifically, the first three PCNM eigenvectors were had the highest variable importance in long-unburned areas and the highest variable importance after time since the last fire among reburned samples. These three PCNM eigenvectors are representative of larger-scale spatial autocorrelation. The FRS score of the sample consistently influenced burn severity in both the long-unburned and reburn models, with higher severity being much more likely with FRS below approximately 0.46 (Fig. 3, Fig. 4). Two variable partial dependence plots showing the probability of high severity fire in previously long-unburned areas (Fig. 5) and in reburns (Figure B.3) indicated that fuel moisture, annual temperature anomalies, annual vapor pressure deficit anomalies, forest structure, and topography were stronger explanatory drivers of variation in burn severity in higher elevation forests where lower fire severity occurred, than in low-elevation dry forests with fire-resistant species.

Daily 1,000-hour fuel moisture was also an important predictor in both models (Fig. 2). In long-unburned areas, daily fire weather had the expected relationship: increased fuel moisture was related to reduced likelihood of high-severity fire. Surprisingly, only daily fuel moisture was retained in predictive models, while other fire weather variables explained little additional variance or were too highly correlated with 1,000-hour daily fuel moisture. Of the annual climate variables, only annual minimum VPD had a clear positive relationship. Prefire basal area was the only forest structure variable retained in both models, and it showed a positive relationship with fire severity. Topographic predictors (slope and TPI) were the among the least important predictors in both models. Unexpectedly, the probability of high-severity fire was higher in flatter than steeper catchments. Relations among variables and the probability of unburned areas were generally opposite those for high-severity (Figure B.1), as would be expected. Unburned areas were clearly associated with lower burning indexes, and with east and west aspects.

In reburns, the time between fires was the most important predictor, and previous burn severity showed a negative relationship with subsequent burn severity. In reburns, high-severity fire likelihood slightly increased 10–18 years after fire (Fig. 4d). High-severity fire likelihood strongly decreased in areas that had previously burned with moderate or high-severity (i.e. RBR > 100). We also observed a strong interaction between the time since past fires and FRS, with very low probabilities of high-severity fire when time since the last fire was < 16 years and the FRS was > 0.5; when FRS was > 0.5 high-severity fire became increasingly likely after 25–28 years (Fig. 6).

In reburns, the probability of high severity consistently increased with daily 1000-hour fuel moisture. This may reflect a narrower range of fuel moisture conditions under which reburns occurred, especially in combination with other predictors (Fig. 6). Biophysical predictors showed similar relationships as for fire in long-unburned areas (e.g., the likelihood of high severity decreased with increasing FRS, and increased with basal area). Within reburns, predictor variables generally showed an opposite relationship with likelihood of being unburned in comparison with the probability of high-severity fire (Figure B.2).

3.2. Influence of prefire and postfire forest management treatments on the burn severity of subsequent fires

All *treatment-fire* samples showed statistically different RBR distributions than those of the paired controls (Table 9). The RBR distributions showed that all treatments except for recent planting displayed

Table 7
Accuracy statistics for RF model predicting burn severity of fires in areas that were previously long-unburned. Cross-validation accuracy = 0.575; Cross-validation Kappa = 0.307; OOB error = 0.305. AUC = area under the receiver operator characteristic curve; AUC C.I. = (95%) confidence interval of the AUC; PPV = positive predictive value; NPV = negative predicted value.

Burn severity class	AUC	AUC C.I.	Sensitivity	Specificity	PPV	NPV	Accuracy
Refugia	0.801	0.793–0.808	0.247	0.969	0.698	0.814	0.805
Low-Moderate	0.702	0.695–0.710	0.481	0.775	0.684	0.596	0.627
High	0.846	0.840–0.852	0.698	0.825	0.597	0.881	0.791

Table 8
Accuracy statistics for RF model predicting burn severity of reburns. Cross validation accuracy = 0.575; Cross-validation Kappa = 0.355; OOB error = 0.280. AUC = area under the receiver operator characteristic curve; AUC C.I. = 95%? confidence interval of the AUC; PPV = positive predictive value; NPV = negative predicted value.

Burn severity class	AUC	AUC C.I.	Sensitivity	Specificity	PPV	NPV	Accuracy
Refugia	0.856	0.845–0.866	0.701	0.831	0.613	0.879	0.795
Low-Moderate	0.772	0.760–0.783	0.394	0.905	0.840	0.540	0.619
High	0.884	0.874–0.895	0.676	0.880	0.524	0.933	0.847

lower burn severity, with the distribution peaks at lower severity values than the controls (Fig. 7). Thinning, thinning + harvest, harvest, harvest + planting, and old planting (≥20 years before the fire) treatments showed strongly overlapping distributions between paired treatments and controls (niche overlap > 0.8), while prescribed fire, and prescribed fire + harvest + planting treatments, had lower overlap of burn severity distributions (niche overlap < 0.54) (Table 9). For treatments that included prescribed fire, the right tail of the distributions was also shifted to lower burn severity values and high-severity fires were uncommon (Fig. 7).

The effect of treatments on decreasing wildfire severity persisted through a second fire, where one occurred. Harvest + planting and planting-alone treatments showed lower severity than reburns with similar time since fire, previous fire severity, fire weather, and bioclimatic setting (Fig. 8). While only two treatments had sufficient samples to be evaluated, the difference between treatments and controls was greater in the *treatment-fire-fire class* (Fig. 7) than in the *treatment-fire class,* meaning that the treatments and the fires had an additive effect on decreasing burn severity in the most recent fire (Fig. 8; Table 9).

Treatments that occurred within 5 years after an initial fire, which were then reburned, did not show as strong a difference in burn severity relative to controls as *treatment-fire* samples revealed (Table 9; Fig. 9). Niche overlap indices for harvest, and harvest + planting treatments were > 0.9 (Table 9). Post-fire harvest + planting and planting-alone treatments experienced less high-severity fire than their paired controls (note the right-tails of the distributions in Fig. 8).

4. Discussion

This study examined factors influencing burn severity across 19 years, 150 fires, and over a large range of forest communities in northeastern Washington state, USA. We found a consistent signal that previous fires—wild or prescribed—and thinning without fire decreased burn severity. Our result for fires in long unburned areas are similar to the results of previous studies modeling burn severity at a given location (e.g., Meigs et al., 2020; Parks et al., 2018a; Povak et al., 2020b), but expand on those studies by highlighting the importance of species traits in determining burn severity, and provide context to our assessment of burn severity in reburns. Our modeling results highlight the importance of spatial autocorrelation, most likely reflecting high spatial autocorrelation in both measured and unmeasured biogeographic drivers of fire severity across different scales, a topic that should be further explored in future research.

4.1. Burn severity in long-unburned areas

Large-scale bioclimatic gradients were the most important drivers of burn severity in long-unburned areas, more so than fire weather, local forest structure, or topography influences. Spatial autocorrelation (as measured by PCNM eigenvectors) and broad patterns of forest resilience to fire (as estimated by the Forest Resilience Score (FRS)), both of which reflect large bioclimatic gradients, were important to predicting the severity of fires that burned previously long-unburned areas. The FRS is associated with the fire resistance traits of species, while other large scale climatic gradients within our study area are associated with the length of the fire season, complexity of topography and land surface forms, and presence of topographic or edaphic barriers to fire spread (Cansler and McKenzie, 2014). Within our study area, FRS was highly correlated with climatic water deficit (*deficit*; Spearman's r = 0.75). Thus, our results correspond with previous research that found AET, deficit, and elevation can be important predictors of burn severity (Dillon et al., 2020; Kane et al., 2015b; Povak et al., 2020b), but contrast with previous studies that found fuel moisture and fire weather variables were the most important predictors (Parks et al., 2018a), and those that highlight the importance of topography (Meigs et al., 2020).

The rather abrupt changes in the probability of high-severity fire along the FRS gradient, and interactions between other variables and FRS (Figs. 6 and 7), indicate that there are distinctive fire regime areas within our study area. While the different fire regimes among different forest communities in the interior Pacific Northwest has long been documented (e.g., Agee, 1996), we see two distinctive fire regimes, one in ponderosa pine and Douglas-fir forests that burned with low-mixed severity and frequent fire prior to Euromerican colonization, and another in higher elevation forests, which where fires were less frequent and tended to burn with higher severity. In the lower-frequency, higher severity fire regimes of the higher-elevation forests, we saw evidence in burn severity was more strongly related to 1000-hour fuel moisture, basal area, slope, and topographical position index. (Fig. 5). The spatial map of FRS we used as a predictor is based on community-scale fire resistance traits, but for interpretation within our study area, we note that 0.46 falls in-between the FRS for *Pseudotsuga menziesii* (0.49) and *Abies grandis* (0.42). FRS was positively correlated with deficit and negatively with elevation in our study area (Fig. 1), but unlike deficit and elevation, FRS has a direct functional relationship to burn severity (Stevens et al., 2020). Plot- and tree-scale empirical modeling have demonstrated the importance of fire-adaptive traits such the bark thickness, lower branch pruning, bud protection, and foliage geometry in determining crown scorch and consumption fire effects (Cansler et al., 2020; Hood et al., 2018; Kane et al., 2013; van Wagtendonk et al., 2020). The FRS provides a useful way to connect functional relationships between species traits and fire effects across broad landscapes.

Previous theoretical work has framed a dichotomy where the spatial controls on fire behavior and effects suddenly shift from controls by means of local fuel and topographic conditions during moderate fire weather, to a collapse of local spatial controls during regionally synchronous drought conditions or severe fire weather events (Kennedy and McKenzie, 2010; McKenzie and Kennedy, 2011, 2012; Povak et al., 2018; Turner and Romme, 1994). Our results support the existence of threshold relationships between the probability of high-severity fire and fuel moisture levels during the burn periods of a fire. We found that low fuel moisture and higher vapor pressure deficit conditions were associated with increased probability of high-severity fire. These modeling results align with earlier research supporting the strong influence of fire weather and annual drought on burn severity in northeastern Washington forests (Cansler and McKenzie, 2014; Parks et al., 2018a). The fire weather data exists at a coarser native resolution (4-km) than the response and predictor data (270-m). Some fire weather variables, such as wind, often vary at a much finer spatial scale than 4-km, and in relation to terrain routing and intensification by topography. Thus, although many fire weather variables were not included in the final model, they may be important at finer scales than we could not resolve with the available data. Annual climate variables, on the other hand, did

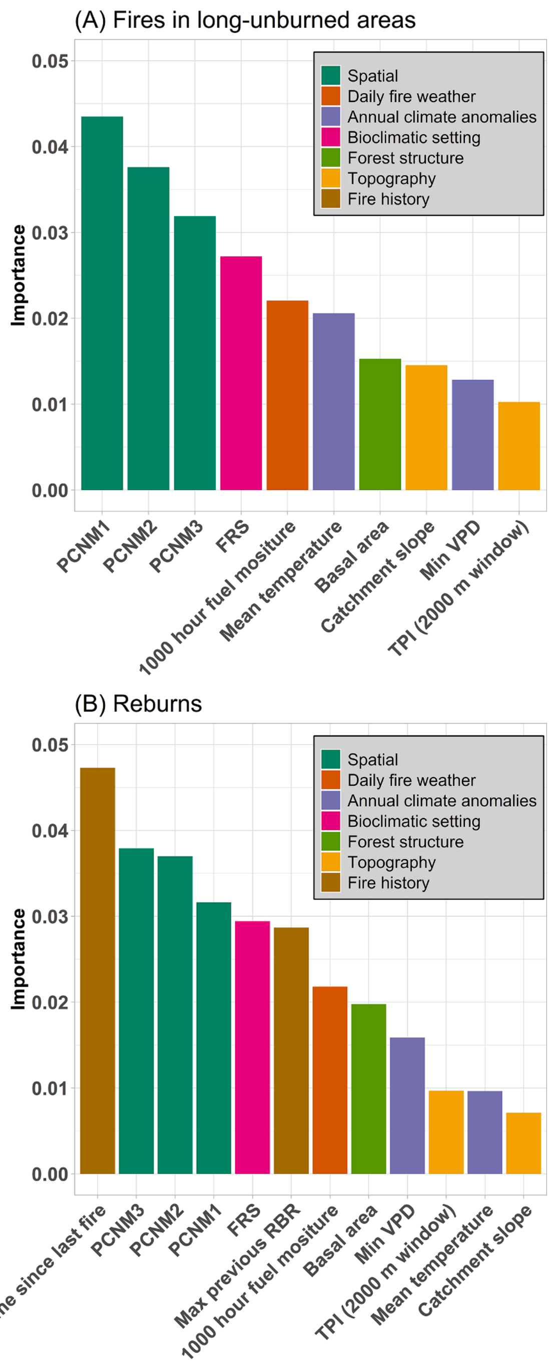

Fig. 2. Variable importance plot from Random Forest models predicting burn severity (relativized burn ratio; RBR) for fire in long-unburned areas (A) and reburns (B). PCNM (principal coordinates of neighborhood matrices) vectors measure spatial autocorrelation with lower-order vectors represent larger-scale spatial autocorrelation, and higher-order vectors represent local-scale spatial autocorrelation. Fire resistance score (FRS) captures community-scale tree species fire resistance traits (Stevens et al., 2020). VPD = annual vapor pressure deficit anomalies. TPI = topographical position index at 2000 m scale. Variable importance is calculate based on how often a variable is used to split predicted outcomes into a correct class. Response data are from wildfires that occurred between 2001 and 2019 in northeastern Washington State, USA. Reburns were previously burned between 1985 and 2018.

not show the consistent relationships with burn severity that we had expected. Specifically, we found that higher temperatures were associated with a lower probability of high-severity fire. In our samples, this could be driven by increased grass and forb growth during cool-wet springs in the lower elevation portions of our study area, resulting in elevated fine fuel loads during summer (Littell et al., 2009). We note that there was multicollinearity between annual temperature anomalies and annual vapor pressure deficit (Spearman's $r = 0.44$), and complex interactions with annual climate that were difficult to interpret. Nevertheless, the negative association between annual temperature anomalies and burn severity was evident even when based on correlation strength (Spearman's $\rho = -0.15$). Some of the recent large fires, such as the 2014 Carlton Complex and 2015 Lime Belt and Tunk Block fires exhibited large daily growth within grasslands and ponderosa pine woodlands. Since wet cool years are associated with grass and forb production in steppe ecosystems in the Inland Pacific Northwest (Littell et al., 2009), it is possible we are seeing an associated between high severity and cool temperature anomalies due to higher fine fuel production in cool years.

Our predictions of unburned areas, corresponded with the definition of temporally varying fire refugia, not long-term "persistent fire refugia" (Meddens et al., 2018). Past research in this region had identified stable, persistent fire refugia that were associated with topographic constraints (Camp et al., 1997). Our initial set of topographical metrics matched recent research in the western Cascades, which used a relatively larger number of topographic metrics when conducting similar modeling of burn severity with the specific goal of identifying fire refugia (Meigs et al., 2020). That research found that north aspects, steep catchments, and concave topographic positions were associated with refugia there. Either (1) our sampling and modeling methods were not targeted enough to identify persistent refugia, or (2) persistent refugia are no longer persistent in the forested parts of northeastern Washington, due to increased landscape flammability due to fire suppression and climatic changes. The later idea is supported by two studies in this region. First, Kolden et al. (2017), found that persistent fire refugia identified by Camp et al. (1997) burned more severely than non-refugia sites in subsequent fires that took places in 2012. Second, Martinez et al. (2019) found relatively little area remained persistently unburned through more than two fires in the Inland Pacific Northwest and Northern Rocky Mountains, USA, and there were relatively little area unburned by two or more fires in northeastern Washington, compared to other parts of their study area. They also found that persistent fire refugia were associated with sparsely vegetated sites (Martinez et al., 2019), which were likely excluded from this study, since we only analyzed areas classified as having forest cover.

4.2. *Reburns*

In reburns the relationships we observed were consistent with the concept of stabilizing (negative) feedbacks (Holling, 1973; Johnstone et al., 2016) in active fire regimes: previous fires consume fuels and thus limit the severity of subsequent fires. Previous fires strongly decreased the severity of subsequent fires (a negative feedback to severe fire) for the first decade after a fire. We did not observe any evidence that prior fires led to higher subsequent burn severity (a positive feedback). We found there was a declining resistance to high-severity with increasing time since fire, with a threshold at about 15 years after the previous fire. The stabilizing feedbacks between initial fires and burn severity in subsequent fires probably reflects increasing fire tolerant species composition and more open canopy structure (Halofsky et al., 2011; Prichard et al., 2017; Stevens-Rumann et al., 2016). In other regions, including the Gila National Forest in New Mexico, the south-central Sierra Nevada and the Klamath Mountains, previous high-severity fires increased the probability of high-severity fire when they reburned more than a decade after the previous fire (Collins et al., 2009; Halofsky et al., 2011; Holden et al., 2010; Thompson et al., 2007), reflecting fast regeneration times of highly flammable sclerophyllous shrubs (Halofsky et al., 2011). Although we have observed large patches of high shrub cover in some in some severely burned areas in northeastern Washington, strong shrub responses are localized, and are generally dominated by shrub species adapted to longer fire rotations (e.g., *Ceanothus*

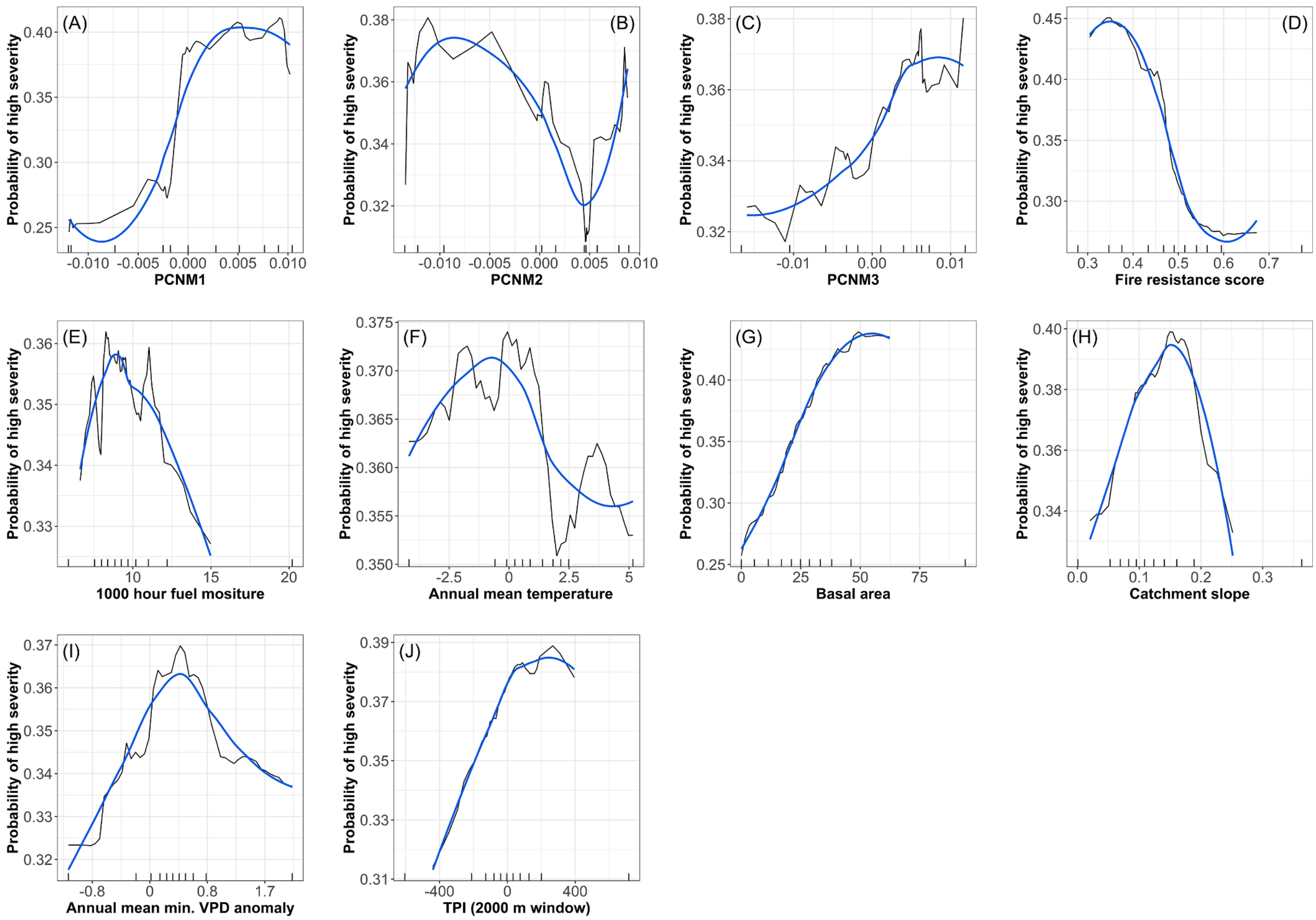

Fig. 3. Partial dependence plots for final random forest model for first-entry fires in long-unburned areas, in northeastern Washington State, occurring between 2001 and 2019. Plots depict the marginal effect of a predictor variable on predicted fire severity. PCNM (principal coordinates of neighborhood matrices) vectors measure spatial autocorrelation with lower-order vectors represent larger-scale spatial autocorrelation, and higher-order vectors represent local-scale spatial autocorrelation. VPD = annual vapor pressure deficit anomalies. TPI = topographical position index at 2000 m scale. Black lines show trends in high severity probability in response to predictors. Blue lines are lowess (locally weighted scatterplot smoothing) of trends in high severity probability in response to predictors. Lines are plotted for the 2–98 percentiles, to remove extreme values. Tick marks on the insides of plots indicted distributions of values for each predictor, with a tick mark at every 10 percentile. Relationships between each predictor and the response, the probability of high severity as measured by the Relativized Burn Ratio (RBR), calculated as partial dependence plots where the values for each predictor are varied throughout their range while values for all other predictors are held to their mean values. As a result, partial dependence plots do not show interactions between predictors, and therefore the change in probabilities on the y-axis does not always correspond with variable importance (Fig. 3). Partial plots for refugia are in Appendix B. (For interpretation of the references to color in this figure legend, the reader is referred to the web version of this article.)

velutinus). We did not see any evidence that species composition, topography, or forest structure exerted stronger controls in reburns than in long-unburned areas, but that may indirectly reflect time since the last fire and previous burn severity because these can be good proxies for surface fuel abundance and vegetation successional development.

High burn severity was most likely to occur in reburns within stands that burned initially with lower severity and that had a low fire resistance score: high elevation subalpine forests where dominant trees species—Engelmann spruce, lodgepole pine, and subalpine fir—have thin bark, flammable foliage, low crown bases, resinous bark and foliage, and undergo little self-pruning of branches (Stevens et al., 2020). Initial fires may have burned with low-severity or skipped those areas entirely during due to discontinuous forest vegetation, high fuel moistures, wet weather during the burning season, or a combination thereof (Cansler et al., 2018; Cansler and McKenzie, 2014).

Our analysis of reburns does not identify places where previous fires stopped the spread of subsequent fires. The probability of high-severity fire was consistently lower in reburns than in long-unburned areas, and the probability of unburned areas was consistently higher, indicating that another stabilizing feedback that were not explicitly testing for—self-limiting fire spread—may also be occurring. In northeastern Washington, fires in the cool-dry forest sometimes stop at the edge of young plantations (Lyons-Tinsley and Peterson, 2012), previous fires (Prichard and Kennedy, 2014), or discontinuous forest cover (Cansler et al., 2018). Self-limiting fire spread has also been documented in the Sierra Nevada, (van Wagtendonk et al., 2012) and the Rocky Mountain Region (Parks et al., 2018c, 2015a; Teske et al., 2012) and elsewhere around the globe (Prichard et al., 2017). Future research in the inland Pacific Northwest could explicitly include areas outside but adjacent to fire perimeters to better understand where and when self-limiting fire spread occurs in this region.

4.3. Scale and burn severity

Measures of spatial autocorrelation were the most important predictors in our models of predicting fire severity in long-unburned areas and reburns. Previous research that included spatial autocorrelation as a predictor variable in fire severity modeling interpreted the finding as revealing effects of contagious disturbance processes, e.g., pre-heating of fuels and improved effectiveness of flame lengths on steep slopes (e.

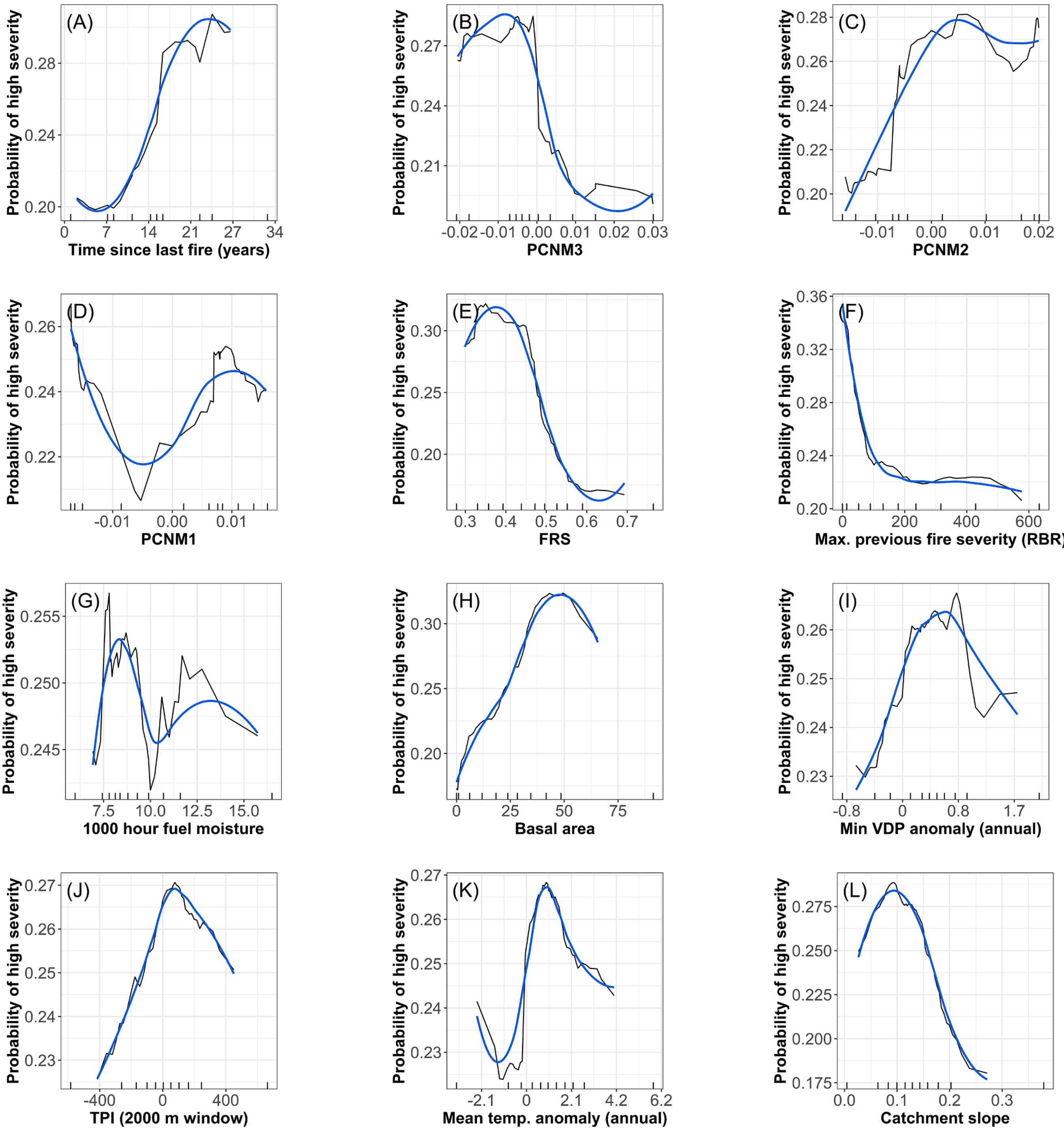

Fig. 4. Partial dependence plots for final random forest model for reburns, in northeastern Washington State, occurring between 2001 and 2019. Plots depict the marginal effect of a predictor variable on predicted fire severity. PCNM (principal coordinates of neighborhood matrices) vectors measure spatial autocorrelation with lower-order vectors represent larger-scale spatial autocorrelation, and higher-order vectors represent local-scale spatial autocorrelation. VPD = annual vapor pressure deficit anomalies. TPI = topographical position index at 2000 m scale. Black lines show trends in high severity probability in response to predictors. Blue lines are lowess (locally weighted scatterplot smoothing) smoothed trend lines of trends in high severity probability in response to predictors. Lines are plotted for the 2–98 percentiles, to remove extreme values. Tick marks on the insides of plots indicted distributions of values for each predictor, with a tick mark at every 10 percentile. Relationships between each predictor and the response, the probability of high severity as measured by the Relativized Burn Ratio (RBR), calculated as partial dependence plots where the values for each predictor are varied throughout their range while values for all other predictors are held to their mean values. As a result, partial dependence plots do not show interactions between predictors. Partial plots for refugia are in Appendix B (For interpretation of the references to color in this figure legend, the reader is referred to the web version of this article.)

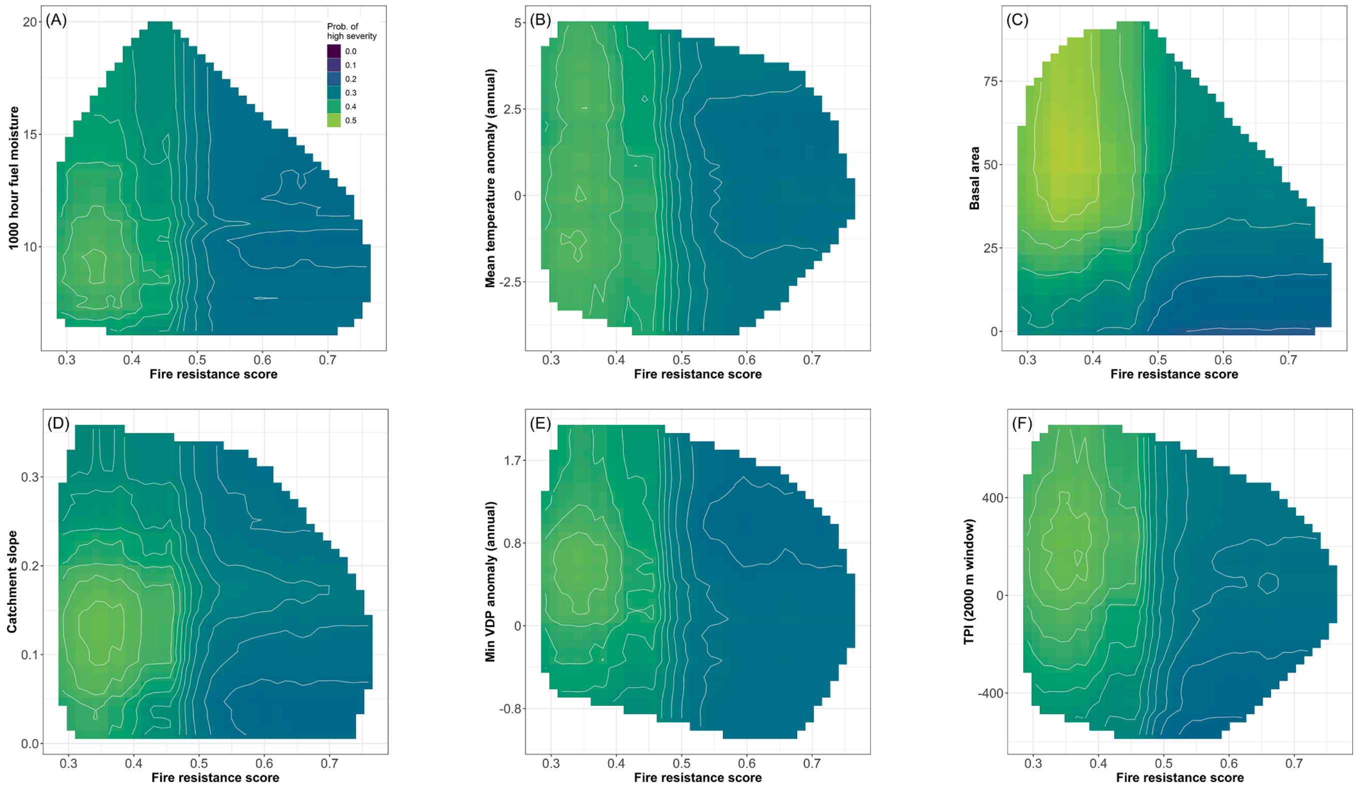

Fig. 5. Two-variable partial dependence surfaces showing probability of high severity fire, as measured by the Relativized Burn Ratio, in areas that were long-unburned before the fire. The most important predictor variables was the fire resistance score (FRS) captures community-scale tree species fire resistance traits (x-axis of each panels; Stevens et al., 2020). VPD = annual vapor pressure deficit anomalies. TPI = topographical position index at 2000 m scale. Fill color indicates a higher probability of high severity, and color ramps in Fig. 6 and Fig. 7 are the same, to aid comparisons. White contour lines are included to aid interpretation. White background with no data indicate there was not sufficient samples of the combination of variables for prediction.

g., Wimberly et al., 2009). In contrast, Povak et al. (2020a) found the variance explained by spatial autocorrelation is mostly duplicative of the variance explained by other environmental variables. Our results are consistent with Povak et al. (2020a) in that large-scale spatial autocorrelation was important in predicting burn severity, not small-scale spatial autocorrelation, which would be indicative of pre-heating of fuels near the flame front. In our models it likely represents large-scale environmental variation that is either unmeasured by the other variables we tested, or multiple environmental drivers operating jointly (Povak et al., 2020b).

We likewise suggest that there is an issue of scale and complexity associated with the extent of our analysis area, which influences which predictor variables have the highest importance in our models. This was a regional analysis, and thus falls between the extent of national fire severity modeling (Dillon et al., 2020) and individual fire modeling (Coen et al., 2018; Povak et al., 2020b). Similar analyses at this ecoregion scale (Dillon et al., 2020; Parks et al., 2018a) have not explored the importance of changing variable sign or interactions, thereby limiting our comparisons to variable importance, not the direction of covariate relations. For example, a machine-learning model developed by Parks et al. (2018a) based on fire severity data from large fires predicted high-severity fire within ecoregions of the US. They found that live fuel moisture and weather, which are combined in our weather variable category, together explained > 55% of the variance in the Okanagan Highlands province, which overlaps our study area, but that study did not show the direction of relationships. We suggest our results indicating complicated or unexpected relationships with annual climate variables, and the low variance explained by some fire weather and topographic metrics that we did not retain in the final models, may reflect analysis of a "middle number domain", where factors operating at a variety of different scales lead to complicated and contingent observed relationships (sensu McKenzie et al., 2011; O'Neill et al., 1986). Alternatively, there may be space and time mismatches, between the coarse spatial resolution daily fire data, coarse temporal resolution annual climate variables, and moderate resolution burn severity response data.

We expect that modeling at the scale of an individual burn period may better elucidate the complex relationships between fuels, weather, and local topography (e.g., Povak et al., 2020b), especially if finer-scale weather data were available. In contrast, modeling at ecoregion or larger scales (e.g., Dillon et al., 2020) may better elucidate relationships with large scale gradients, such as species distributions and relative abundance and associated energy and water limitations on vegetation structure and composition. Explicitly investigating how the importance of variables changes when modeling is conducted at different spatial domains could lead to better model interpretation and identification of the most relevant scales for prediction application.

4.4. Management implications

The contribution of this study is that it demonstrates the strong effects of previous wildfire and prescribed fire on subsequent fire severity across a large landscape and multiple forest types, many fire years, and wide ranges of climate and weather. We found that management treatments that include prescribed fire were most effective at decreasing the severity of subsequent fires. These results are consistent with previous research in our study area (Agee and Lolley, 2006; Lyons-Tinsley and Peterson, 2012; Prichard et al., 2020; Prichard and Kennedy, 2014), and elsewhere in western North America (Kalies and Yocom Kent, 2016; Schwilk et al., 2009; Stephens and Moghaddas, 2005), but our sampled area encompasses > 7,000 sampled 30-m areas in the entire reburned landscape (51,919 ha; Table 6), and all 3,086 ha within prescribed fire areas that were subsequently burned by a wildfire, instead of field plots

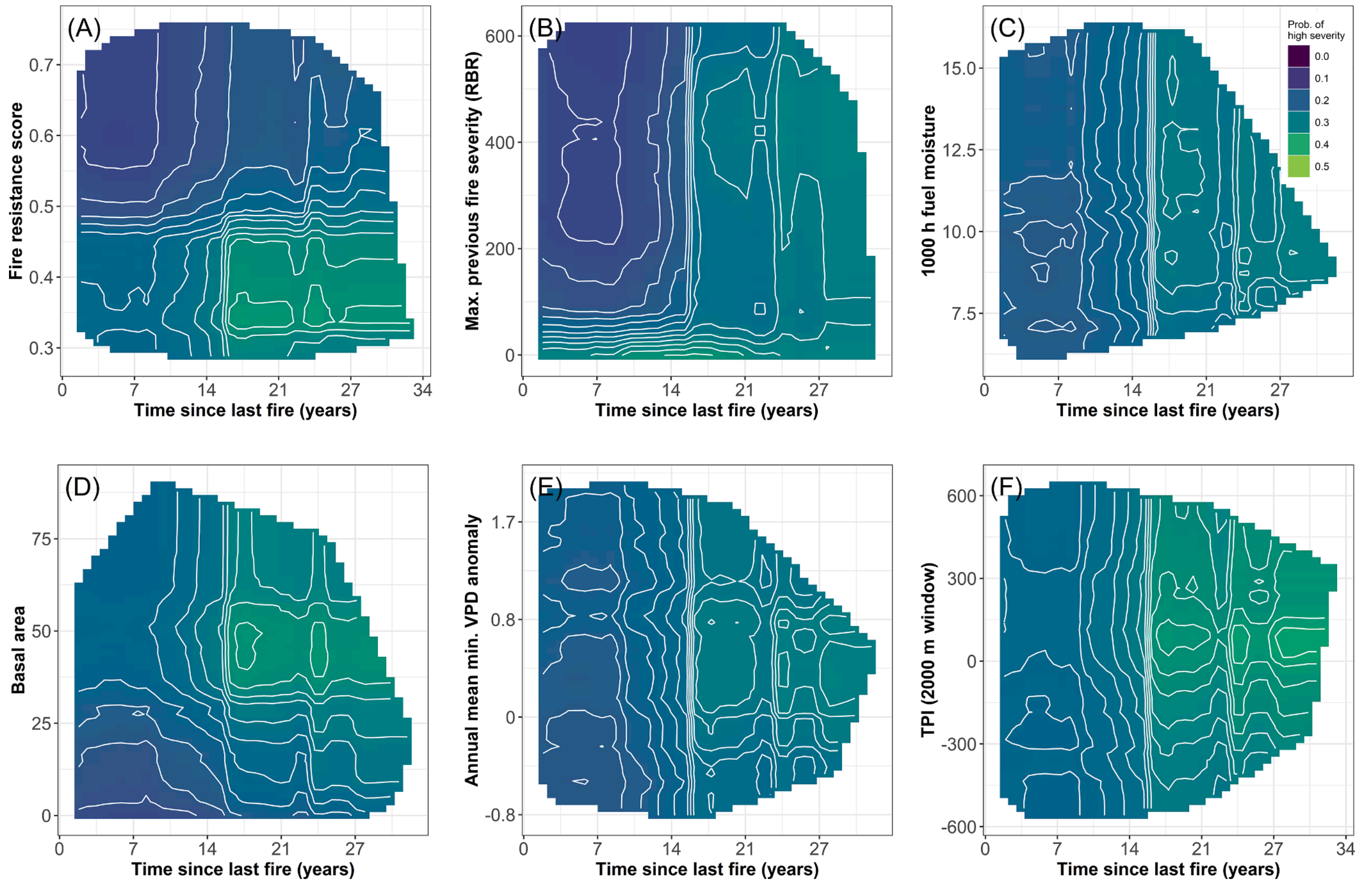

Fig. 6. Two-variable partial dependence surfaces showing probability of high severity fire, as measured by the Relativized Burn Ratio, in areas that were reburned. The most important predictor variables in reburns was the years since the last fire (x-axis). VPD = annual vapor pressure deficit anomalies. TPI = topographical position index at 2000 m scale. Fill color indicates a higher probability of high severity, and color ramps in Fig. 6 and Fig. 7 are the same, to aid comparisons. White areas with no data indicate there was not sufficient samples of the combination of variables to confidently predict the relationship.

Table 9
Niche overlap and two-sample Kolmogorov–Smirnov (K-S test) results for *treatment-fires* and postfire pre-reburn treatments. Wildfires occurred from 2001 to 2018, and treatments took place from 1982 to 2017. In reburns, first fires occurred from 1985 to 2014, and reburns occurred between 2001 and 2018. Sample sizes subsamples used in the statistical analysis are provided in Table 6.

Treatment	Niche overlap	D (test statistic)	*P*-value
Treatment-fires			
Thinning	0.810	0.170	<0.001
Thinning and harvest	0.536	0.476	<0.001
Harvest	0.794	0.211	<0.001
Harvest and planting	0.790	0.215	<0.001
Planting (old; ≥20 years before fire)	0.850	0.158	<0.001
Planting (recent; ≤10 years before fire)	0.842	0.148	<0.001
Prescribed fire	0.628	0.377	<0.001
Prescribed fire and harvest	0.520	0.489	<0.001
Prescribed fire, harvest, and planting	0.476	0.535	<0.001
Treatment-fire-fire			
Harvest and planting	0.734	0.272	<0.001
Planting	0.733	0.258	<0.001
Fire-treatment-fire			
Harvest	0.855	0.155	<0.001
Harvest and planting	0.823	0.092	<0.001
Planting	0.759	0.252	<0.001

sampling small portions of the landscape. Our prescribed fire treatments results are compelling not only because they caused a decrease in overall burn severity, but also almost completely prevented high-severity fire. Thus, prescribed fire sets up a strong stabilizing feedback, increasing resilience to subsequent fires.

Most of the other treatments, including thinning, and harvest combined with planting also decreased the severity of fires occurring in long-unburned areas. These treatments likely decreased fire severity by decreasing horizontal and vertical fuel continuity. These results too are supported by previous research indicating that thinning alone can moderate fire behavior, in our study area (Prichard et al., 2020; Prichard and Kennedy, 2014). But across western North America, the combination of thinning and prescribed fire is most effective at moderating fire behavior and reducing fire severity (Fulé et al., 2012; Kalies and Yocom Kent, 2016; Martinson and Omi, 2013; Prichard et al. 2021, Schwilk et al., 2009). We also found that harvest treatments burned with higher severity than paired controls, which is consistent with previous research showing that harvest operations can increase surface fuel loads when tree limbs and tops are relocated to surface fuel beds, resulting in higher fire severity (Prichard and Kennedy, 2012; Stephens et al., 2009). Further insights may be gained from research at ecoregion scales to specifically identify the sets of conditions when thinning and prescribed fire are not effective at reducing fire severity.

When recent plantings burned, they often burned with higher severity, most likely due to the lack of fire resistant traits of young conifers: thin bark and low crow bases result in more severe fire injury in small conifers (Agee, 1996; Cansler et al., 2020; Hood et al., 2018). Previous research has found both positive (Zald and Dunn, 2018) and negative (Lyons-Tinsley and Peterson, 2012) associations between young stands and burn severity. Post-fire planting, along or in other combination with other management, is best implemented with on-the-

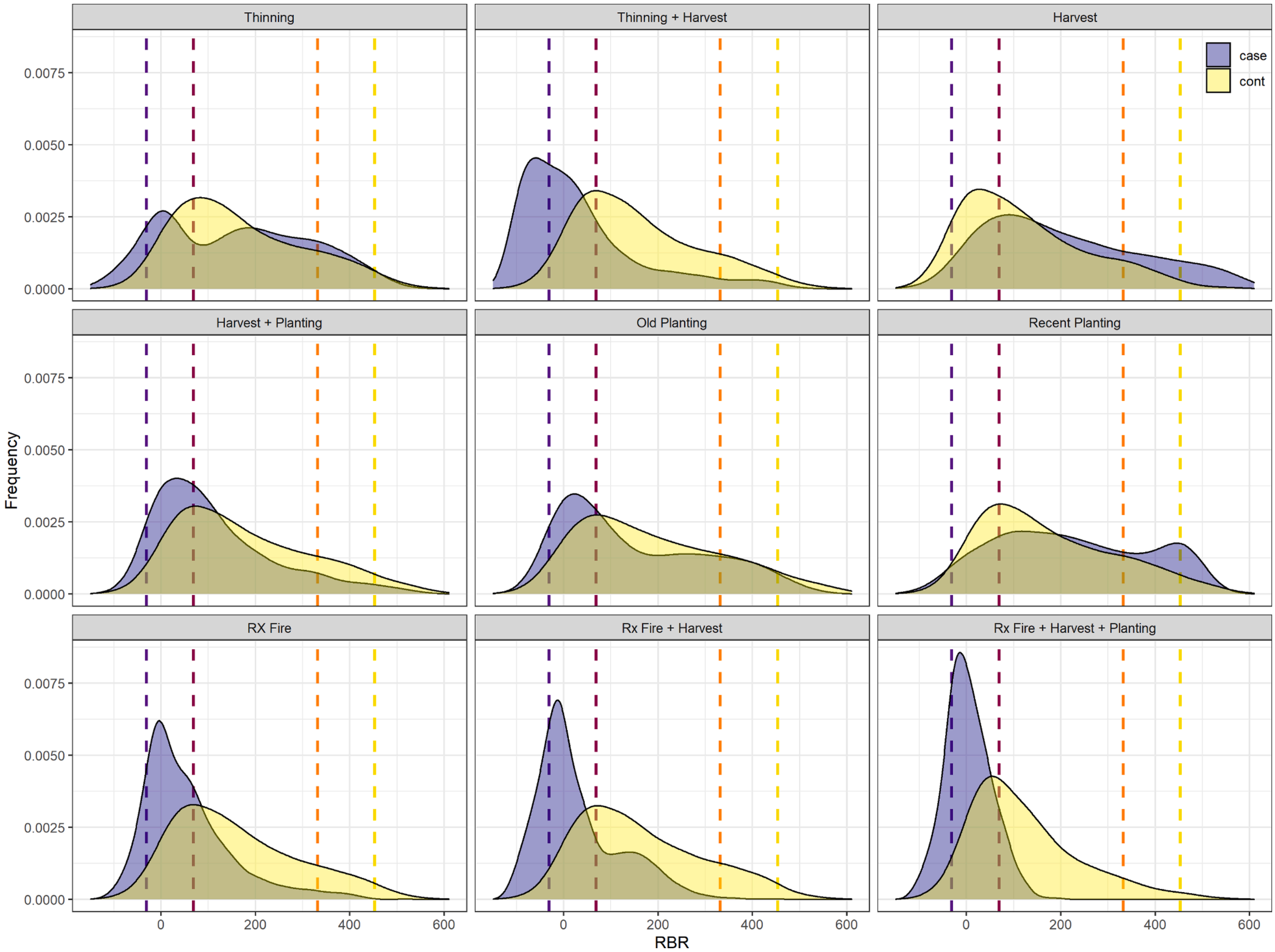

Fig. 7. Burn severity distributions for areas treated then burned (i.e., "treatment-fire") and untreated burned controls. Density plots showing the frequency distribution of the Relativized Burn Ratio (RBR), a measurement of burn severity, for untreated areas (controls; yellow) and silvicultural or fuel treatment (cases; purple) in areas that were treated before a wildfire. Vertical dashed lines show the thresholds: <2% basal area loss (dark purple), unburned-low and moderate severity (magenta), low-moderate and high severity mixes (orange), and >98% basal area mortality (i.e., stand replacing severity; yellow). Data are from wildfires that occurred between 2001 and 2018 and treatments occurring from 1982 to 2017, within the northeastern Washington State, USA study area. (For interpretation of the references to color in this figure legend, the reader is referred to the web version of this article.)

ground practices that matched the natural regeneration dynamics of the forest community (Stevens et al., 2022), as well as in locations that account for larger-scale landscape priorities (Churchill et al., 2022), and expected future climate and fire regimes (Larson et al., 2022). We did not see evidence for increase burn severity in plantings that took place after an initial fire and then subsequently reburned (Fig. 7). Therefore, we reiterate the findings of Lyons-Tinsley and Peterson (2012): treatment of surface fuels before planting occurs provides an important dampening effects on subsequent burn severity in young plantations in northeastern Washington.

5. Conclusions

Species composition across large bioclimatic gradients had the strongest influence of fire severity in long-unburned areas in northeastern Washington, USA. Previous wildfires, prescribed fires, and management treatments functioned as stabilizing feedbacks, decreasing the severity of subsequent fires. If managers wish to decrease the severity of subsequent fires, then their best tools are (1) prescribed fire treatments and (2) allowing fires to burn under moderate weather conditions. Managers can also use thinning to decrease the severity of subsequent fires but thinning combined with prescribed fire is most effective (cf. Johnston et al., 2021). Planting, in contrast, could either increase or decrease burn severity, depending on the timing of subsequent fires and whether post-harvest slash is properly burned. We did not find any evidence for amplifying feedbacks that have been observed in other regions (Halofsky et al., 2011; Harvey et al., 2016) between the severity of initial fires and subsequent fires. Here, high-severity was less likely in areas that pervious burned with high-severity. Our results strongly support the moderating influences of previous wildfires, harvest, thinning, and especially prescribed burns on the severity of subsequent wildfires.

CRediT authorship contribution statement

C. Alina Cansler: Conceptualization, Methodology, Resources, Writing – original draft, Writing – review & editing, Supervision, Formal analysis, Visualization. **Van R. Kane:** Conceptualization, Methodology, Writing – review & editing, Supervision, Project administration. **Paul F. Hessburg:** Conceptualization, Writing – original draft, Writing – review & editing, Project administration. **Jonathan T. Kane:** Methodology, Validation, Formal analysis, Data curation, Visualization. **Sean M.A. Jeronimo:** Methodology, Data curation, Writing – review & editing. **James A. Lutz:** Resources, Conceptualization, Writing – original draft,

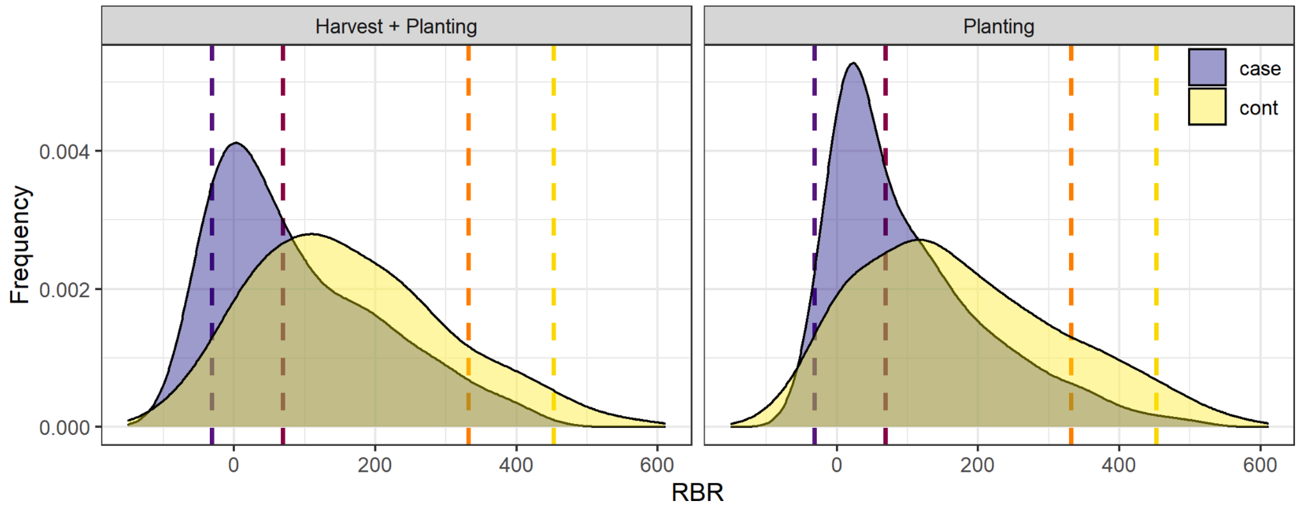

Fig. 8. Burn severity distributions from reburns in areas treated then burned by two fire (i.e., "*treatment-fire-fire*") and untreated burned controls. Distributions show the severity of the second fire, Density plots showing the frequency distribution of the Relativized Burn Ratio (RBR), a measurement of burn severity, for untreated areas (controls; yellow) and each silviculture or fuel treatment (cases; purple), for equally-sized match subsamples in areas that were treated before fire. Vertical dashed lines correspond with the following thresholds: <2% basal area loss (dark purple), refugia-low and moderate severity (magenta), low-moderate and high severity (orange), and > 98% basal area mortality (i.e., stand replacing severity; yellow). Data are from wildfires that occurred between 2001 and 2018, and treatments occurring from 1982 to 2017, within initial fires occurring from 1985 to 2017. (For interpretation of the references to color in this figure legend, the reader is referred to the web version of this article.)

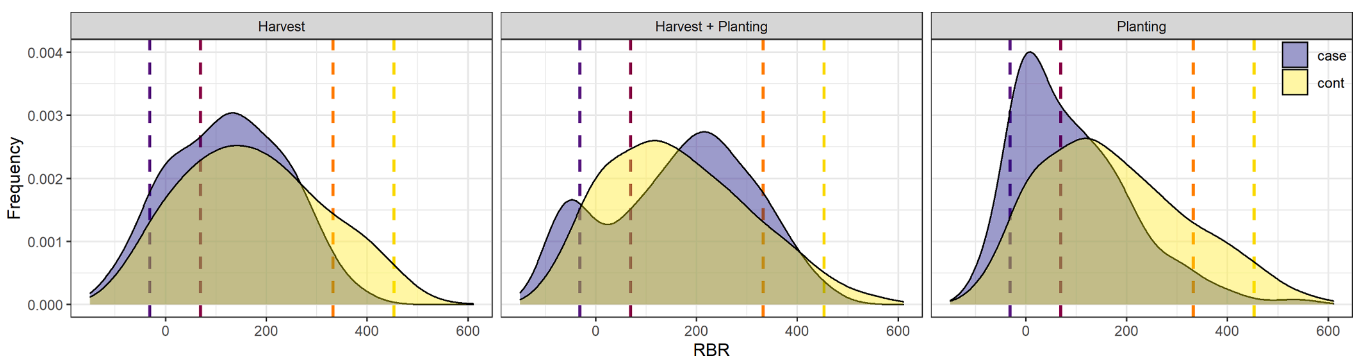

Fig. 9. Areas that were burned, treated, then reburned (i.e., *fire-treatment-*fire) and untreated controls burn severity distributions or the reburns. Density plots showing the frequency distribution of the Relativized Burn Ratio (RBR), a measurement of burn severity, for untreated areas (controls; yellow) and each silviculture or fuel treatment (cases; purple), for equally-sized match subsamples in areas that were treated before fire. Vertical dashed lines correspond with the following thresholds: <2% basal area loss (dark purple), refugia-low and moderate severity (magenta), low-moderate and high severity (orange), and >98% basal area mortality (i.e., stand replacing severity; yellow). Data are from wildfires that occurred between 2001 and 2018, and treatments occurring from 1982 to 2017, within initial fires occurring from 1985 to 2017. (For interpretation of the references to color in this figure legend, the reader is referred to the web version of this article.)

Writing – review & editing. **Nicholas A. Povak:** Methodology, Conceptualization, Writing – review & editing. **Derek J. Churchill:** Conceptualization, Writing – review & editing. **Andrew J. Larson:** Supervision, Project administration, Funding acquisition, Conceptualization, Writing – original draft, Writing – review & editing.

Declaration of Competing Interest

The authors declare that they have no known competing financial interests or personal relationships that could have appeared to influence the work reported in this paper.

Acknowledgements

Funding was provided by Joint Fire Science Program Project ID: 16-1-05-24. We appreciate comments from two anonymous reviewers that improved the manuscript.

Appendix A. Supplementary data

Supplementary data to this article can be found online at https://doi.org/10.1016/j.foreco.2021.119764.

References

Abatzoglou, J.T., 2013. Development of gridded surface meteorological data for ecological applications and modelling. Int. J. Climatol. 33 (1), 121–131. https://doi.org/10.1002/joc.v33.110.1002/joc.3413.
Abatzoglou, J.T., Williams, A.P., 2016. Impact of anthropogenic climate change on wildfire across western US forests. Proc. Natl. Acad. Sci. U. S. A. 113 (42), 11770–11775. https://doi.org/10.1073/pnas.1607171113.
Agee, J.K., 1998. The landscape ecology of western forest fire regimes. Northwest Sci. 72, 24–34.
Agee, J.K., 1996. Fire Ecology of Pacific Northwest Forests. Island Press, Washington DC.
Agee, J.K., Lolley, M.R., 2006. Thinning and Prescribed Fire Effects on Fuels and Potential Fire Behavior in an Eastern Cascades Forest, Washington, USA. Fire Ecol. 2 (2), 3–19. https://doi.org/10.4996/fireecology.0202003.
Agee, J.K., Skinner, C.N., 2005. Basic principles of forest fuel reduction treatments. For. Ecol. Manage. 211 (1-2), 83–96. https://doi.org/10.1016/j.foreco.2005.01.034.
Boehmke, B., Greenwell, B., 2019. Hands-On Machine Learning with R. Chapman and Hall/CRC. https://doi.org/10.1201/9780367816377.

Borcard, D., Legendre, P., 2002. All-scale spatial analysis of ecological data by means of principal coordinates of neighbour matrices. Ecol. Modell. 153 (1-2), 51–68. https://doi.org/10.1016/S0304-3800(01)00501-4.

Bradley, A.P., 1997. The use of the area under the ROC curve in the evaluation of machine learning algorithms. Pattern Recognit. 30 (7), 1145–1159. https://doi.org/10.1016/S0031-3203(96)00142-2.

Breiman, L., 2001. Random forests. Mach. Learn. 45, 5–32. https://doi.org/10.1023/A:1010933404324.

Burcsu, T., Halofsky, J., Bisrat, S., 2014. Dynamic vegetation modeling of forest, woodland, shrubland, and grassland vegetation communities in the Pacific Northwest and Southwest Regions of the United States, in: Halofsky, J.E., Creutzburg, M.K., Hemstrom, M. (Eds.), Integrating Social, Economic, and Ecological Values across Large Landscapes. Gen. Tech. Rep. PNW-GTR-896. US Department of Agriculture, Forest Service, Pacific Northwest Research Station, Portland, OR, pp. 15–70.

Brenning, A., Bangs., D., 2016. RSAGA: SAGA geoprocessing and terrain analysis in R. R package version 0.94-5. http://CRAN.R-project.org/package=RSAGA.

Camp, A., Oliver, C., Hessburg, P., Everett, R., 1997. Predictinglate-successional fire refugia pre-dating European settlement in the Wenatchee mountains. For. Ecol. Manage. 95 (1), 63–77. https://doi.org/10.1016/S0378-1127(97)00006-6.

Cansler, C.A., Hood, S.M., van Mantgem, P.J., Varner, J.M., 2020. A large database supports the use of simple models of post-fire tree mortality for thick-barked conifers, with less support for other species. Fire Ecol. 16, 25. https://doi.org/10.1186/s42408-020-00082-0.

Cansler, C.A., McKenzie, D., 2012. How robust are burn severity indices when applied in a new region? Evaluation of alternate field-based and remote-sensing methods. Remote Sens. 4, 456–483. https://doi.org/10.3390/rs4020456.

Cansler, C.A., McKenzie, D., Halpern, C.B., 2018. Fire enhances the complexity of forest structure in alpine treeline ecotones: Ecosphere 9 (2), e02091. https://doi.org/10.1002/ecs2.2018.9.issue-210.1002/ecs2.2091.

Cansler, C.A., McKenzie, D., 2014. Climate, fire size, and biophysical setting control fire severity and spatial pattern in the northern Cascade Range. USA. Ecol. Appl. 24 (5), 1037–1056. https://doi.org/10.1890/13-1077.1.

Chen, C., Liaw, A., Breiman, L., 2004. Using Random Forest to Learn Imbalanced Data. Discov. Stat. Univ. California, Berkeley, CA, Tech. Rep, pp. 666. 1–12.

Churchill, D.J., Larson, A.J., Dahlgreen, M.C., Franklin, J.F., Hessburg, P.F., Lutz, J.A., 2013. Restoring forest resilience: From reference spatial patterns to silvicultural prescriptions and monitoring. For. Ecol. Manage. 291, 442–457. https://doi.org/10.1016/j.foreco.2012.11.007.

Churchill, D.J., Jeronimo, S.M.A., Hessburg, P.F., Cansler, C.A., Povak, N.A., Kane, V.R., Lutz, J.A., Larson, A.J., 2022. Post-fire landscape evaluations in Eastern Washington, USA: Assessing the Work of Contemporary Wildfires. For. Ecol. Manage. https://doi.org/10.1016/j.foreco.2021.119796 (in press).

Coen, J.L., Stavros, E.N., Fites-Kaufman, J.A., 2018. Deconstructing the King megafire. Ecol. Appl. 28 (6), 1565–1580. https://doi.org/10.1002/eap.1752.

Collins, B.M., Miller, J.D., Thode, A.E., Kelly, M., van Wagtendonk, J.W., Stephens, S.L., 2009. Interactions among wildland fires in a long-established Sierra Nevada natural fire area. Ecosystems 12 (1), 114–128. https://doi.org/10.1007/s10021-008-9211-7.

Conover, W.J., Iman, R.L., 1981. Rank Transformations as a Bridge Between Parametric and Nonparametric Statistics. Am. Stat. 35 (3), 124–129.

Daly, C., Gibson, W.P., Taylor, G.H., Johnson, G.L., Pasteris, P., 2002. A knowledge-based approach to the statistical mapping of climate. Clim. Res. 22, 99–113. https://doi.org/10.3354/cr022099.

Daly, C., Halbleib, M., Smith, J.I., Gibson, W.P., Doggett, M.K., Taylor, G.H., Curtis, J., Pasteris, P.P., 2008. Physiographically sensitive mapping of climatological temperature and precipitation across the conterminous United States. Int. J. Climatol. 28 (15), 2031–2064. https://doi.org/10.1002/joc.v28:1510.1002/joc.1688.

Daly, C., Neilson, R.P., Phillips, D.L., 1994. A Statistical-Topographic Model for Mapping Climatological Precipitation over Mountainous Terrain. J. Appl. Meteorol. 33, 140–158. https://doi.org/10.1175/1520-0450(1994)033<0140:ASTMFM>2.0.CO;2.

Dillon, G.K., Panunto, M.H., Davis, B., Morgan, P., Birch, D.S., Jolly, W.M., 2020. Development of a severe fire potential map for the contiguous United States. USDA For. Serv. - Gen. Tech. Rep. RMRS-GTR 2020, 1–107.

Dobrowski, S.Z., Abatzoglou, J., Swanson, A.K., Greenberg, J.A., Mynsberge, A.R., Holden, Z.A., Schwartz, M.K., 2013. The climate velocity of the contiguous United States during the 20th century. Glob. Chang. Biol. 19 (1), 241–251. https://doi.org/10.1111/gcb.12026.

Dray, S., Legendre, P., Peres-Neto, P.R., 2006. Spatial modelling: a comprehensive framework for principal coordinate analysis of neighbour matrices (PCNM). Ecol. Modell. 196 (3-4), 483–493. https://doi.org/10.1016/j.ecolmodel.2006.02.015.

Eidenshink, J., Schwind, B., Brewer, K., Zhu, Z.-L., Quayle, B., Howard, S., 2007. A Project for Monitoring Trends in Burn Severity. Fire Ecol. 3 (1), 3–21. https://doi.org/10.4996/fireecology.0301003.

Fulé, P.Z., Crouse, J.E., Roccaforte, J.P., Kalies, E.L., 2012. Do thinning and/or burning treatments in western USA ponderosa or Jeffrey pine-dominated forests help restore natural fire behavior? For. Ecol. Manage. 269, 68–81. https://doi.org/10.1016/j.foreco.2011.12.025.

Furniss, T.J., Kane, V.R., Larson, A.J., Lutz, J.A., 2020. Detecting tree mortality with Landsat-derived spectral indices: Improving ecological accuracy by examining uncertainty. Remote Sens. Environ. 237, 111497. https://doi.org/10.1016/j.rse.2019.111497.

Greenwell, B.M., 2017. pdp: An R package for constructing partial dependence plots. R J. 9, 421–436. https://doi.org/10.32614/rj-2017-016.

Hagmann, R.K., Hessburg, P.F., Prichard, S.J., Povak, N.A., Brown, P.M., Fulé, P.Z., Keane, R.E., Knapp, E.E., Lydersen, J.M., Metlen, K.L., Reilly, M.J., Sánchez Meador, A.J., Stephens, S.L., Stevens, J.T., Taylor, A.H., Yocom, L.L., Battaglia, M.A., Churchill, D.J., Daniels, L.D., Falk, D.A., Henson, P., Johnston, J.D., Krawchuk, M.A., Levine, C.R., Meigs, G.W., Merschel, A.G., North, M.P., Safford, H.D., Swetnam, T. W., Waltz, A.E.M., 2021. Evidence for widespread changes in the structure, composition, and fire regimes of western North American forests. Ecological Applications. https://doi.org/10.1002/eap.2431.

Halofsky, J.E., Donato, D.C., Hibbs, D.E., Campbell, J.L., Cannon, M.D., Fontaine, J.B., Thompson, J.R., Anthony, R.G., Bormann, B.T., Kayes, L.J., Law, B.E., Peterson, D.L., Spies, T.A., 2011. Mixed-severity fire regimes: lessons and hypotheses from the Klamath-Siskiyou Ecoregion. Ecosphere 2 (4), art40. https://doi.org/10.1890/ES10-00184.1.

Harvey, B.J., Donato, D.C., Turner, M.G., 2016. Burn me twice, shame on who? Interactions between successive forest fires across a temperate mountain region. Ecology 97 (9), 2272–2282. https://doi.org/10.1002/ecy.1439.

Haugo, R.D., Kellogg, B.S., Cansler, C.A., Kolden, C.A., Kemp, K.B., Robertson, J.C., Metlen, K.L., Vaillant, N.M., Restaino, C.M., 2019. The missing fire: quantifying human exclusion of wildfire in Pacific Northwest forests, USA. Ecosphere 10, e02702. https://doi.org/10.1002/ecs2.2702.

Hessburg, P.F., Agee, J.K., 2003. An environmental narrative of Inland Northwest United States forests, 1800–2000. For. Ecol. Manage. 178 (1-2), 23–59. https://doi.org/10.1016/S0378-1127(03)00052-5.

Hessburg, P.F., Agee, J.K., Franklin, J.F., 2005. Dry forests and wildland fires of the inland Northwest USA: Contrasting the landscape ecology of the pre-settlement and modern eras, in: Forest Ecology and Management. https://doi.org/10.1016/j.foreco.2005.02.016.

Hessburg, P.F., Churchill, D.J., Larson, A.J., Haugo, R.D., Miller, C., Spies, T.A., North, M.P., Povak, N.A., Belote, R.T., Singleton, P.H., Gaines, W.L., Keane, R.E., Aplet, G.H., Stephens, S.L., Morgan, P., Bisson, P.A., Rieman, B.E., Salter, R.B., Reeves, G.H., 2015. Restoring fire-prone Inland Pacific landscapes: seven core principles. Landsc. Ecol. 30 (10), 1805–1835. https://doi.org/10.1007/s10980-015-0218-0.

Hessburg, P.F., Miller, C.L., Parks, S.A., Povak, N.A., Taylor, A.H., Higuera, P.E., Prichard, S.J., North, M.P., Collins, B.M., Hurteau, M.D., Larson, A.J., Allen, C.D., Stephens, S.L., Rivera-Huerta, H., Stevens-Rumann, C.S., Daniels, L.D., Gedalof, Z., Gray, R.W., Kane, V.R., Churchill, D.J., Hagmann, R.K., Spies, T.A., Cansler, C.A., Belote, R.T., Veblen, T.T., Battaglia, M.A., Hoffman, C., Skinner, C.N., Safford, H.D., Salter, R.B., 2019. Climate, environment, and disturbance history govern resilience of western North American forests. Front. Ecol. Evol. 7 (239) https://doi.org/10.3389/fevo.2019.00239.

Hessburg, P.F., Prichard, S.J., Hagmann, R.K., Povak, N.A., Lake, F.K., 2021. Wildfire and climate change adaptation of western North American forests: a case for intentional management. Ecol. Appl. https://doi.org/10.1002/eap.2432.

Hessburg, P.F., Smith, B.G., Salter, R.B., Ottmar, R.D., Alvarado, E., 2000. Recent changes (1930s–1990s) in spatial patterns of interior northwest forests. USA. For. Ecol. Manage. 136, 53–83. https://doi.org/10.1007/BF00125134.

Hijmans, R.J., van Etten, J., 2012. raster: Geographic analysis and modeling with raster data. R package version 2.0-12. http://CRAN.R-project.org/package=raster.

Holden, Z.A., Morgan, P., Hudak, A.T., 2010. Burn severity of areas reburned by wildfires in the gila national forest, New Mexico, USA. Fire Ecol. 6 (3), 77–85. https://doi.org/10.4996/fireecology.0603085.

Holden, Z.A., Swanson, A., Luce, C.H., Jolly, W.M., Maneta, M., Oyler, J.W., Warren, D. A., Parsons, R., Affleck, D., 2018. Decreasing fire season precipitation increased recent western US forest wildfire activity. Proc. Natl. Acad. Sci. U. S. A. 115 (36), E8349–E8357. https://doi.org/10.1073/pnas.1802316115.

Holling, C.S., 1973. Resilience and Stability of Ecological Systems. Annu. Rev. Ecol. Syst. 4 (1), 1–23. https://doi.org/10.1146/annurev.es.04.110173.000245.

Hood, S.M., Varner, J.M., van Mantgem, P., Cansler, C.A., 2018. Fire and tree death: understanding and improving modeling of fire-induced tree mortality. Environ. Res. Lett. 13 (11), 113004. https://doi.org/10.1088/1748-9326/aae934.

Hosmer, David W., Lemeshow, S., Sturdivant, Rodney X., 2000. *Applied logistic regression*. Wiley, New York.

Johnston, J.D., Olszewski, J.H., Miller, B.A., Schmidt, M.R., Vernon, M.J., Ellsworth, L. M., 2021. Mechanical thinning without prescribed fire moderates wildfire behavior in an Eastern Oregon, USA ponderosa pine forest. For. Ecol. Manage. 501, 119674. https://doi.org/10.1016/j.foreco.2021.119674.

Johnstone, J.F., Allen, C.D., Franklin, J.F., Frelich, L.E., Harvey, B.J., Higuera, P.E., Mack, M.C., Meentemeyer, R.K., Metz, M.R., Perry, G.LW., Schoennagel, T., Turner, M.G., 2016. Changing disturbance regimes, ecological memory, and forest resilience. Front. Ecol. Environ. 14 (7), 369–378. https://doi.org/10.1002/fee.1311.

Kalies, E.L., Yocom Kent, L.L., 2016. Tamm Review: Are fuel treatments effective at achieving ecological and social objectives? A systematic review. For. Ecol. Manage. 375, 84–95. https://doi.org/10.1016/j.foreco.2016.05.021.

Kane, V.R., Bartl-Geller, B.N., North, M.P., Kane, J.T., Lydersen, J.M., Jeronimo, S.M.A., Collins, B.M., Monika Moskal, L., 2019. First-entry wildfires can create opening and tree clump patterns characteristic of resilient forests. For. Ecol. Manage. 454, 117659. https://doi.org/10.1016/j.foreco.2019.117659.

Kane, V.R., Cansler, C.A., Povak, N.A., Kane, J.T., McGaughey, R.J., Lutz, J.A., Churchill, D.J., North, M.P., 2015a. Mixed severity fire effects within the Rim fire: Relative importance of local climate, fire weather, topography, and forest structure. For. Ecol. Manage. 358, 62–79. https://doi.org/10.1016/j.foreco.2015.09.001.

Kane, V.R., Lutz, J.A., Cansler, C.A., Povak, N.A., Churchill, D.J., Smith, D.F., Kane, J.T., North, M.P., 2015b. Water balance and topography predict fire and forest structure patterns. For. Ecol. Manage. 338, 1–13. https://doi.org/10.1016/j.foreco.2014.10.038.

Kane, V.R., Lutz, J.A., Roberts, S.L., Smith, D.F., McGaughey, R.J., Povak, N.A., Brooks, M.L., 2013. Landscape-scale effects of fire severity on mixed-conifer and red fir forest structure in Yosemite National Park. For. Ecol. Manage. 287, 17–31. https://doi.org/10.1016/j.foreco.2012.08.044.

Kennedy, M.C., McKenzie, D., 2010. Using a stochastic model and cross-scale analysis to evaluate controls on historical low-severity fire regimes. Landsc. Ecol. 25 (10), 1561–1573. https://doi.org/10.1007/s10980-010-9527-5.

Key, C.H., 2006. Ecological and sampling constraints on defining landscape fire severity. Fire Ecol. 2 (2), 34–59. https://doi.org/10.4996/fireecology.0202034.

Kolden, C., Bleeker, T., Smith, A., Poulos, H., Camp, A., 2017. Fire effects on historical wildfire refugia in contemporary wildfires. Forests 8 (10), 400. https://doi.org/10.3390/f8100400.

Kuhn, M., 2008. Building predictive models in R Using the caret package. J. Stat. Softw. 28, 1–26. https://doi.org/10.18637/jss.v028.i05.

Larson, A.J., Jeronimo, S.M.A., Hessburg, P.F., Lutz, James A., Povak, N.A., Cansler, C.A., Kane, V.R., Churchill, D.J., 2022. Ecological Principles to Guide Post-Fire Forest Landscape Management in the Inland Pacific. For. Ecol. Manage. https://doi.org/10.1016/j.foreco.2021.119680 (in press).

Littell, J.S., McKenzie, D., Peterson, D.L., Westerling, A.L., 2009. Climate and wildfire area burned in western U.S. ecoprovinces, 1916–2003. Ecol. Appl. 19 (4), 1003–1021. https://doi.org/10.1890/07-1183.1.

Lutz, J.A., Van Wagtendonk, J.W., Franklin, J.F., 2009. Twentieth-century decline of large-diameter trees in Yosemite National Park, California, USA. For. Ecol. Manage. 257 (11), 2296–2307. https://doi.org/10.1016/j.foreco.2009.03.009.

Lyons-Tinsley, C., Peterson, D.L., 2012. Surface fuel treatments in young, regenerating stands affect wildfire severity in a mixed conifer forest, eastside Cascade Range, Washington. USA. For. Ecol. Manage. 270, 117–125. https://doi.org/10.1016/j.foreco.2011.04.016.

Mallek, C., Safford, H., Viers, J., Miller, J., 2013. Modern departures in fire severity and area vary by forest type, Sierra Nevada and southern Cascades, California, USA. Ecosphere 4, 1–28. https://doi.org/10.1890/ES13-00217.1.

Marsaglia, G., Tsang, W.W., Wang, J., 2003. Evaluating Kolmogorov's distribution. J. Stat. Softw. 8, 1–4. https://doi.org/10.18637/jss.v008.i18.

Martinez, A.J., Meddens, A.J.H., Kolden, C.A., Strand, E.K., Hudak, A.T., 2019. Characterizing persistent unburned islands within the Inland Northwest USA. Fire Ecol. 15 (1) https://doi.org/10.1186/s42408-019-0036-x.

Martinson, E.J., Omi, P.N., 2013. Fuel treatments and fire severity: A meta-analysis. USDA For. Serv. - Res. Pap. RMRS-RP 1–38.

McGaughey, R.J., 2021. FUSION/LDV: Software for LIDAR data analysis and visualization. FUSION Version 4, 20. http://forsys.cfr.washington.edu/FUSION/fusion_overview.html.

McKenzie, D., Kennedy, M.C., 2012. Power laws reveal phase transitions in landscape controls of fire regimes. Nat. Commun. 3 (1) https://doi.org/10.1038/ncomms1731.

McKenzie, D., Kennedy, M.C., 2011. Scaling Laws and Complexity in Fire Regimes. In: McKenzie, D.A., Miller, C., Falk, D.A. (Eds.), The Landscape Ecology of Fire. Ecological Studies (Analysis and Synthesis). Springer, Netherlands, Dordrecht, pp. 27–49. https://doi.org/10.1007/978-94-007-0301-8_2.

McKenzie, D., Miller, C., Falk, D.A., 2011. Toward a Theory of Landscape Fire, in: D., M., C., M., D., F. (Eds.), The Landscape Ecology of Fire. Ecological Studies (Analysis and Synthesis). Springer, Dordrecht, pp. 3–25. https://doi.org/10.1007/978-94-007-0301-8_1.

Meddens, A.J.H., Kolden, C.A., Lutz, J.A., Smith, A.M.S., Cansler, C.A., Abatzoglou, J.T., Meigs, G.W., Downing, W.M., Krawchuk, M.A., 2018. Fire refugia: What are they, and why do they matter for global change? Bioscience 68, 944–954. https://doi.org/10.1093/biosci/biy103.

Meigs, G.W., Dunn, C.J., Parks, S.A., Krawchuk, M.A., 2020. Influence of topography and fuels on fire refugia probability under varying fire weather conditions in forests of the pacific northwest. USA. Can. J. For. Res. 50 (7), 636–647. https://doi.org/10.1139/cjfr-2019-0406.

Meyer, D., Dimitriadou, E., Hornik, K., Weingessel, A., Leisch, F., 2020. e1071: Misc Functions of the Department of Statistics, Probability Theory Group (Formerly: E1071), TU Wien. R package version 1.7-4. https://CRAN.R-project.org/package=e1071.

Millar, C.I., Stephenson, N.L., Stephens, S.L., 2007. Climate change and forests of the future: Managing in the face of uncertainty. Ecol. Appl. 17 (8), 2145–2151. https://doi.org/10.1890/06-1715.1.

O'Neill, R.V., Deangelis, D.L., Waide, J.B., Allen, T.F., Allen, G.E., 1986. A hierarchical concept of ecosystems, No. 23. Princeton University Press.

Ohmann, J.L., Gregory, M.J., 2002. Predictive mapping of forest composition and structure with direct gradient analysis and nearest-neighbor imputation in coastal Oregon, U.S.A. Can. J. For. Res. 32 (4), 725–741. https://doi.org/10.1139/x02-011.

Oksanen, A.J., Blanchet, F.G., Friendly, M., Kindt, R., Legendre, P., Mcglinn, D., Minchin, P.R., Hara, R.B.O., Simpson, G.L., Solymos, P., Stevens, M.H.H., Szoecs, E., Wagner, H., 2019. vegan: Community Ecology Package. R package version 2.5-6. https://CRAN.R-project.org/package=vegan.

Parisien, M.-A., Barber, Q.E., Hirsch, K.G., Stockdale, C.A., Erni, S., Wang, X., Arseneault, D., Parks, S.A., 2020. Fire deficit increases wildfire risk for many communities in the Canadian boreal forest. Nat. Commun. 11 (1) https://doi.org/10.1038/s41467-020-15961-y.

Parks, S.A., 2021. Personal Communicaiton, May 6, 2021. https://code.earthengine.google.com/c76157be827be2f24570df50cca427e9.

Parks, S.A., 2014. Mapping day-of-burning with coarse-resolution satellite fire-detection data. Int. J. Wildl. Fire 23, 215–223. https://doi.org/10.1071/WF13138.

Parks, S.A., Abatzoglou, J.T., 2020. Warmer and drier fire seasons contribute to increases in area burned at high severity in Western US forests from 1985 to 2017. Geophys. Res. Lett. 47, 1–10. https://doi.org/10.1029/2020GL089858.

Parks, S.A., Dillon, G.K., Miller, C., 2014. A new metric for quantifying burn severity: The relativized burn ratio. Remote Sens. 6, 1827–1844. https://doi.org/10.3390/rs6031827.

Parks, S.A., Holsinger, L.M., Miller, C., Nelson, C.R., 2015a. Wildland fire as a self-regulating mechanism: The role of previous burns and weather in limiting fire progression. Ecol. Appl. 25 (6), 1478–1492. https://doi.org/10.1890/14-1430.110.1890/14-1430.1.sm.

Parks, S.A., Holsinger, L.M., Panunto, M.H., Jolly, W.M., Dobrowski, S.Z., Dillon, G.K., 2018a. High-severity fire: Evaluating its key drivers and mapping its probability across western US forests. Environ. Res. Lett. 13 (4), 044037. https://doi.org/10.1088/1748-9326/aab791.

Parks, S., Holsinger, L., Voss, M., Loehman, R., Robinson, N., 2018b. Mean composite fire severity metrics computed with Google Earth Engine offer improved accuracy and expanded mapping potential. Remote Sens 10 (6), 879. https://doi.org/10.3390/rs10060879.

Parks, S.A., Miller, C., Parisien, M.-A., Holsinger, L.M., Dobrowski, S.Z., Abatzoglou, J., 2015b. Wildland fire deficit and surplus in the western United States, 1984–2012. Ecosphere 6 (12), art275. https://doi.org/10.1890/ES15-00294.110.1890/ES15-00294.1.sm.

Parks, S.A., Parisien, M.-A., Miller, C., Holsinger, L.M., Baggett, L.S., 2018c. Fine-scale spatial climate variation and drought mediate the likelihood of reburning. Ecol. Appl. 28 (2), 573–586. https://doi.org/10.1002/eap.1671.

Povak, N.A., Churchill, D.J., Cansler, C.A., Hessburg, P.F., Kane, V.R., Kane, J.T., Lutz, J.A., Larson, A.J., 2020a. Wildfire severity and postfire salvage harvest effects on long-term forest regeneration. Ecosphere 11 (8). https://doi.org/10.1002/ecs2.v11.810.1002/ecs2.3199.

Povak, N.A., Hessburg, P.F., Salter, R.B., 2018. Evidence for scale-dependent topographic controls on wildfire spread. Ecosphere 9 (10). https://doi.org/10.1002/ecs2.2018.9.issue-1010.1002/ecs2.2443.

Povak, N.A., Kane, V.R., Collins, B.M., Lydersen, J.M., Kane, J.T., 2020b. Multi-scaled drivers of severity patterns vary across land ownerships for the 2013 Rim Fire. California. Landsc. Ecol. 35 (2), 293–318. https://doi.org/10.1007/s10980-019-00947-z.

Prichard, S.J., Hessburg, P.F., Hagmann, R.K., Povak, N.A., Dobrowski, S.Z., Hurteau, M.D., Kane, V.R., Keane, R.E., Kobziar, L.N., Kolden, C.A., North, M., Parks, S.A., Safford, H.D., Stevens, J.T., Yocom, L.L., Churchill, D.J., Gray, R.W., Huffman, D.W., Lake, F.K., Khatri-Chhetri, P., 2021. Adapting western North American forests to climate change and wildfires: ten common questions. Ecological Applications. https://doi.org/10.1002/eap.2433.

Prichard, S.J., Kennedy, M.C., 2014. Fuel treatments and landform modify landscape patterns of burn severity in an extreme fire event. Ecol. Appl. 24 (3), 571–590. https://doi.org/10.1890/13-0343.1.

Prichard, S.J., Kennedy, M.C., 2012. Fuel treatment effects on tree mortality following wildfire in dry mixed conifer forests, Washington State, USA. Int. J. Wildl. Fire 21, 1004–1013. https://doi.org/10.1071/WF11121.

Prichard, S.J., Povak, N.A., Kennedy, M.C., Peterson, D.W., 2020. Fuel treatment effectiveness in the context of landform, vegetation, and large, wind-driven wildfires. Ecol. Appl. 30, 1–22. https://doi.org/10.1002/eap.2104.

Prichard, S.J., Stevens-Rumann, C.S., Hessburg, P.F., 2017. Tamm Review: Shifting global fire regimes: Lessons from reburns and research needs. For. Ecol. Manage. 396, 217–233. https://doi.org/10.1016/j.foreco.2017.03.035.

Priestley, C.H.B., Taylor, R.J., 1972. On the assessment of surface heat flux and evaporation using large-scale parameters. Mon. Weather Rev. 100, 81–92. https://doi.org/10.1175/1520-0493(1972)100<0081:OTAOSH>2.3.CO;2.

Qiu Y, M.J., 2018. RSpectra: Solvers for Large-Scale Eigen- value and SVD Problems.

R Core Team, 2020. R: A language and environment for statistical computing. R Foundation for Statistical Computing, Vienna, Austria https://www.R-project.org/.

Robin, X., Turck, N., Hainard, A., Tiberti, N., Lisacek, F., Sanchez, J.C., Müller, M., 2011. pROC: an open-source package for R and S+ to analyze and compare ROC curves. BMC Bioinformatics 8, 12–77.

Saberi, S., Harvey, B.J., 2021. Do you CBI what I see? The relationship between the Composite Burn Index and quantitative field measures of burn severity varies across gradients of forest structure. Int. J. Wildl, Fire In revisio.

Saberi, S., Harvey, B., Cansler, C.A., Smith, A., 2020. Professional communication between University of Washington scientists and Washington Department of Natural Resources scientists; Severity Thresholds for Washington and Oregon. October 8, 2020.

Saberi, S.J., 2019. Quantifying burn severity in forests of the interior Pacific Northwest: From field measurements to satellite spectral indices. University of Washington.

Schuurman, G.W., Hoffman, C.H., Cole, D.N., Lawrence, D.J., Morton, J.M., Magness, D.R., Cravens, A.E., Covington, S., O'Malley, R., Fisichelli, N.A., 2020. Resist-Accept-Direct (RAD)— A Framework for the 21st-century Natural Resource Manager. Fort Collins, Colorado.

Schwilk, D.W., Keeley, J.E., Knapp, E.E., McIver, J., Bailey, J.D., Fettig, C.J., Fiedler, C.E., Harrod, R.J., Moghaddas, J.J., Outcalt, K.W., Skinner, C.N., Stephens, S.L., Waldrop, T.A., Yaussy, D.A., Youngblood, A., 2009. The national Fire and Fire Surrogate study: Effects of fuel reduction methods on forest vegetation structure and fuels. Ecol. Appl. 19 (2), 285–304. https://doi.org/10.1890/07-1747.1.

Stephens, S.L., Moghaddas, J.J., 2005. Fuel treatment effects on snags and coarse woody debris in a Sierra Nevada mixed conifer forest. For. Ecol. Manage. 214 (1-3), 53–64. https://doi.org/10.1016/j.foreco.2005.03.055.

Stephens, S.L., Moghaddas, J.J., Edminster, C., Fiedler, C.E., Haase, S., Harrington, M., Keeley, J.E., Knapp, E.E., McIver, J.D., Metlen, K., Skinner, C.N., Youngblood, A., 2009. Fire treatment effects on vegetation structure, fuels, and potential fire severity in western U.S. forests. Ecol. Appl. 19 (2), 305–320. https://doi.org/10.1890/07-1755.1.

Stephenson, N., 1998. Actual evapotranspiration and deficit: Biologically meaningful correlates of vegetation distribution across spatial scales. J. Biogeogr. 25 (5), 855–870. https://doi.org/10.1046/j.1365-2699.1998.00233.x.

Stevens, J.T., Haffey, C.M., Coop, J.D., Fornwalt, P.J., Yocom, L., Allen, C.D., Bradley, A., Bradley, O.T., Carril, D., Chambers, M.E., Chapman, T.B., Haire, S.L., Hurteau, M.D., Iniguez, J.M., Margolis, E.Q., Marks, C., Marshall, L.A.E., Rodman, K.C., Stevens-Rumann, C.S., Thode, A.E., Walker, J.J., 2022. Postfire landscape management in frequent-fire conifer forests of the southwestern United States. For. Ecol. Manage. https://doi.org/10.1016/j.foreco.2021.119678 (in press).

Stevens-Rumann, C.S., Prichard, S.J., Strand, E.K., Morgan, P., 2016. Prior wildfires influence burn severity of subsequent large fires. Can. J. For. Res. 46 (11), 1375–1385. https://doi.org/10.1139/cjfr-2016-0185.

Stevens, J.T., Collins, B.M., Miller, J.D., North, M.P., Stephens, S.L., 2017. Changing spatial patterns of stand-replacing fire in California conifer forests. For. Ecol. Manage. 406, 28–36. https://doi.org/10.1016/j.foreco.2017.08.051.

Stevens, J.T., Kling, M.M., Schwilk, D.W., Varner, J.M., Kane, J.M., Gillespie, T., 2020. Biogeography of fire regimes in western U.S. conifer forests: A trait-based approach. Glob. Ecol. Biogeogr. 29 (5), 944–955. https://doi.org/10.1111/geb.v29.510.1111/geb.13079.

Teske, C.C., Seielstad, C.A., Queen, L.P., 2012. Characterizing fire-on-fire interactions in three large wilderness areas. Fire Ecol. 8 (2), 82–106. https://doi.org/10.4996/fireecology.0802082.

Thompson, J.R., Spies, T.A., Ganio, L.M., 2007. Reburn severity in managed and unmanaged vegetation in a large wildfire. Proc. Natl. Acad. Sci. U. S. A. 104 (25), 10743–10748. https://doi.org/10.1073/pnas.0700229104.

Turner, M.G., Romme, W.H., 1994. Landscape dynamics in crown fire ecosystems. Landsc. Ecol. 9 (1), 59–77. https://doi.org/10.1007/BF00135079.

van Wagtendonk, J.W., Moore, P.E., Yee, J.L., Lutz, J.A., 2020. The distribution of woody species in relation to climate and fire in Yosemite National Park, California, USA. Fire Ecol. 16 (1) https://doi.org/10.1186/s42408-020-00079-9.

van Wagtendonk, J.W., van Wagtendonk, K.A., Thode, A.E., 2012. Factors associated with the severity of intersecting fires in Yosemite National Park, California, USA. Fire Ecol. 8 (1), 11–31. https://doi.org/10.4996/fireecology.0801011.

Vose, J.M., Peterson, D.L., Domke, G.M., Fettig, C.J., Joyce, L.A., Keane, R.E., Luce, C.H., Prestemon, J.P., Band, L.E., Clark, J.S., Cooley, N.E., D'Amato, A., Halofsky, J.E., 2018. Forests, in: Reidmiller, D.R., Avery, C.W., Easterling, D.R., Kunkel, K.E., Lewis, K.L.M., Maycock, T.K., Stewart, B.C. (Eds.), Impacts, Risks, and Adaptation in the United States: The Fourth National Climate Assessment, Volume II. Washington, DC, pp. 232–267. https://doi.org/10.7930/NCA4.2018.CH6.

WADNR, 2020. Forest health assessment and treatment framework (RCW 76.06.200), 1255.

Wang, T., Hamann, A., Spittlehouse, D., Carroll, C., Álvarez, I., 2016. Locally downscaled and spatially customizable climate data for historical and future periods for North America. PLoS One 11 (6), e0156720. https://doi.org/10.1371/journal.pone.0156720.

Westerling, A.L., 2016. Increasing western US forest wildfire activity: Sensitivity to changes in the timing of spring. Philos. Trans. R. Soc. B Biol. Sci. 371 (1696), 20150178. https://doi.org/10.1098/rstb.2015.0178.

Wickham, H., Averick, M., Bryan, J., Chang, W., McGowan, L., François, R., Grolemund, G., Hayes, A., Henry, L., Hester, J., Kuhn, M., Pedersen, T., Miller, E., Bache, S., Müller, K., Ooms, J., Robinson, D., Seidel, D., Spinu, V., Takahashi, K., Vaughan, D., Wilke, C., Woo, K., Yutani, H., 2019. Welcome to the Tidyverse. J. Open Source Softw. 4, 1686. https://doi.org/10.21105/joss.01686.

Wilson, B.T., Lister, A.J., Riemann, R.I., Griffith, D.M., 2013. Live tree species basal area of the contiguous United States (2000-2009) [Data], in: USDA Research Data Archive. USDA Forest Service, Rocky Mountain Research Station, Newtown Square, PA., p. https://www.fs.usda.gov/rds/archive/Catalog/RDS-20. https://doi.org/https://doi.org/10.2737/RDS-2013-0013.

Wimberly, M.C., Cochrane, M.A., Baer, A.D., Pabst, K., 2009. Assessing fuel treatment effectiveness using satellite imagery and spatial statistics. Ecol. Appl. 19 (6), 1377–1384. https://doi.org/10.1890/08-1685.1.

Wright, M.N., Ziegler, A., 2015. ranger: A fast implementation of random forests for high dimensional data in C++ and R. arXiv preprint arXiv:1508.04409.

Zald, H.S.J., Dunn, C.J., 2018. Severe fire weather and intensive forest management increase fire severity in a multi-ownership landscape. Ecol. Appl. 28 (4), 1068–1080. https://doi.org/10.1002/eap.2018.28.issue-410.1002/eap.1710.